CHARACTERIZATION OF RBL2 IN MUSCLE STEM CELL FATE DECISIONS

LUCAS CAMPAGNA

A THESIS SUBMITTED TO
THE FACULTY OF GRADUATE STUDIES
IN PARTIAL FUFILLMENT OF THE REQUIREMENTS
FOR THE DEGREE OF
MASTER OF SCIENCE

GRADUATE PROGRAM IN KINESIOLOGY AND HEALTH SCIENCE
YORK UNIVERSITY
TORONTO, ONTARIO

OCTOBER, 2023

Abstract

Skeletal muscle stem cells (MuSCs) regenerate muscle upon injury. Here, they receive activation signals from their environment and make a fate decision to make further copies (self-renew) or commit to becoming muscle (differentiate). Dysfunctional MuSC fate decisions, lead to poor muscle quality. Accordingly, retinoblastoma-like protein 2 (Rbl2) was characterized in MuSC fate decisions. Targeted deletion of Rbl2 in muscle progenitors impaired myotube formation, demonstrating its potential requirement for MuSC function. Rbl2 was analyzed during MuSC fate decisions by immunostaining cultured myofibers with Pax7 and MyoD. Rbl2 was expressed in the nucleus of only a fraction of committed MuSCs. Surprisingly, during a differentiation time course, primary myogenic progenitor cells expressed Rbl2 in the mitochondria. The Rbl2 expression in the mitochondria of differentiating MuSCs was confirmed in vivo by immunohistochemistry. These results provide novel insights for the localization of Rbl2 in MuSC fate decisions and the mechanisms driving differentiation.

Acknowledgements

This endeavor would not have been possible without the collective effort, guidance and support from my community of advisors, lab mates, family and friends, who have all made sacrifices to ensure the completion of this thesis. This body of knowledge is a product of your sacrifices, and reflects my growth as a researcher and individual.

I would like to express sincere gratitude towards my supervisor **Dr. Anthony Scimè**, for providing me the opportunity to pursue my love for science. Your curiosity and enthusiasm for learning and discovery is something that I admire and has fueled my journey. Importantly, you contributed endlessly with new ideas, encouragement and counsel throughout this entire degree. I appreciate the countless hours you have spent to help make this research come to life.

I would like to extend my appreciation to **Dr. Olasunkanmi Adegoke** for being a part of my supervisory committee and for continuing to support my education and endeavours. In addition, I want to thank **Dr. Tara Haas** for her guidance and for providing essential research materials that contributed to this thesis.

To my current and former lab mates, **Justin**, **Vicky**, **Michelle**, **Joy**, and **Mark**, thank you all for taking time out of your busy schedules to teach and assist me. You have all been a significant part of my journey and your efforts are appreciated immensely. I am very lucky to work with you.

To my loving **parents**, **sister**, **extended family,** and **friends**, I am forever grateful for your sacrifices and willingness to help me succeed in all the ways that you can. To my loving girlfriend **Kira,** words cannot describe my appreciation for all that you do to help support my dreams. Thank you all for making this a reality and for your contributions to science.

Statement of Contributions

All writing, graphic designs and experimental analyses were performed by **Lucas Campagna** under the advice and supervision of **Dr. Anthony Scimè**. Edits were provided by **Dr. Anthony Scimè, Dr. Olasunkanmi Adegoke** and **Dr. Tara Haas.** For muscle regeneration experiments, femoral artery ligation surgeries were conducted by **George Nader** and longitudinal sections were prepared and cut by **Mark Danesh**. All other experiments were performed by **Lucas Campagna**. Experiment materials were provided by **Dr. Anthony Scimè** and **Dr. Tara Haas**.

Table of Contents

List of Figures

Chapter 1:

Literature Review:

Chapter 4:

Results:

List of Abbreviations

ADP	Adenosine diphosphate
ATP	Adenosine triphosphate
α-Tub	Alpha-Tubulin
BAX	Bcl-2-like protein 4
BSA	Bovine Serum Albumin
CDK	Cyclin-dependent kinase
CoQ	Ubiquinone
Cox4	Cytochrome c oxidase
Ctl	Control
CytC	Cytochrome c
DAPI	4′,6-diamidino-2 phenylindole
DMEM	Dulbecco's Modified Eagle's Medium
DMD	Duchenne muscular dystrophy
DNA	Deoxyribonucleic acid
DRP1	Dynamin-related protein 1
EDL	Extensor digitorum longus
$FADH_2$	Reduced flavin adenine dinucleotide
FBS	Fetal Bovine Serum
FFA	Free fatty acid
GA	Growth arrest
GFP	Green fluorescent protein
IMM	Inner mitochondrial membrane

IMS	Intermembrane space
KO	Knockout
LRC	Label-retaining cell
MPC	Myogenic progenitor cell
MRF	Myogenic regulatory factor
MRF4	Myogenic regulatory factor 4
mtDNA	Mitochondrial deoxyribonucleic acid
mTORC1	Mammalian target of rapamycin complex 1
MuSCs	Muscle stem cells
MyHC	Myosin heavy chain
Myf5	Myogenic factor 5
MyoD	Myoblast determination protein 1
MyoG	Myogenin
NADH	Reduced nicotinamide adenine dinucleotide
OMM	Outer mitochondrial membrane
OPA1	Optic atrophy-1
OXPHOS	Oxidative phosphorylation
Pax7	Paired homeobox transcription factor 7
PBS	Phosphate buffered saline
P/S	Penicillin/Streptomycin
PFA	Paraformaldehyde
Pitx2	Paired-like homeodomain transcription factor 2
Pitx3	Paired-like homeodomain transcription factor 3

PMF	Proton motive force
Pro	Proliferating
Rb	Retinoblastoma susceptibility
Rb1	Retinoblastoma associated protein 1
Rbl1	Retinoblastoma-like protein 1
Rbl2	Retinoblastoma-like protein 2
RC	Reserve cell
ROS	Reactive oxygen species
sgRNA	Single guide ribonucleic acid
TBS	Tris-buffered saline
TBST	Tris-buffered saline and Triton X-100
TCA	Tricarboxylic acid
TA	Tibialis anterior

CHAPTER 1

LITERATURE REVIEW

1.1 Adult skeletal muscle stem cells

Skeletal muscle is an essential tissue of study for the following reasons. First, it comprises a relatively large portion of human body mass (about 40%) and contains 50-75% of all body proteins (Frontera & Ochala, 2015). Second, skeletal muscle is essential for mechanical action, regulating body movement through the coordinated contraction of multinucleated muscle fibers. Third, skeletal muscle contributes to the regulation of metabolic activity, storing and oxidizing substrates to be used for energy production (Frontera & Ochala, 2015). Fourth, notably skeletal muscle has the remarkable capacity to regenerate after injury. This regenerative ability depends on a subset of muscle stem cells (MuSCs) (Dumont et al., 2015a).

The MuSCs reside between the basal lamina and plasma membrane of skeletal muscle fibers (Mauro, 1961), providing an optimal zone to access signals from the environment and to integrate into existing fibers to form new muscle. MuSCs were first characterized in 1961 through electron microscopic imaging and were termed “satellite cells” in reference to their observed peripheral location on muscle fibers (Mauro, 1961). MuSCs make up approximately 30% to 35% of myonuclei at birth and these proportions drastically decrease with age to as little as approximately 2% of total myonuclei (White et al., 2010). The importance of MuSCs for skeletal muscle regeneration and maintenance has been highlighted in studies that have genetically deleted essential regulatory elements and transcription factors for normal MuSC functioning. For example, genetic deletion of the paired homeobox transcription factor 7 (Pax7) which characterizes quiescent MuSCs, results in severe muscle wasting and kyphosis in aged mice, an approximately 50% reduction in myonuclei per muscle fiber, precocious differentiation, a reduction in

regenerated muscle fibers, and in most cases death within 2-3 weeks post birth (Seale et al., 2000; Kuang et al., 2006; Mansouri et al., 1996; Von Maltzahn et al., 2013).

The importance of MuSCs in skeletal muscle regeneration and maintenance is also evident during age related and muscle wasting diseases, where there is abnormal MuSC functioning. Sarcopenia is defined as the age related decline in muscle mass, strength and function that is accompanied with distinct cellular and metabolic alterations (Cruz-Jentoft & Sayer, 2019). MuSC number and function decline in aged muscle (Hwang & Brack, 2018). There is increased MuSC commitment at the expense of self-renewal, increased apoptosis, and senescence, which contribute to a reduction in the number of MuSCs and regenerative potential with age (Price et al., 2014; Chakkalakal et al., 2012; Cosgrove et al., 2014; Conboy et al., 2005).

MuSC function is crucial to muscular dystrophies, which are inherited muscular diseases defined by muscle wasting and weakness caused by several described gene mutations (Emery, 2002; Mercuri et al., 2019). The most common of the dystrophies, Duchenne muscular dystrophy (DMD), caused by mutations in the dystrophin gene, exhibits altered MuSC function (Mercuri et al., 2019; Filippelli & Chang, 2021). Here, there is a reduced ability of dystrophin-deficient MuSCs to commit to the myogenic program that is needed for sufficient muscle regeneration (Dumont et al., 2015b). Furthermore, MuSCs in DMD display increased senescence and accelerated differentiation (Sugihara et al., 2020; Yablonka-Reuveni & Anderson, 2006).

1.2 Muscle stem cell fate decisions

Muscle is a highly plastic tissue, owing to the regenerative capacity of resident MuSCs and their ability to make fate decisions to either self-renew or commit to differentiate into muscle (Bianconi & Mozzetta, 2022). In healthy adult muscle, MuSCs are maintained in a mitotically quiescent state (Dumont et al., 2015c). One essential regulatory factor that characterizes quiescent

MuSCs is their expression of Pax7 (**Fig. 1.1**) (Zammit et al., 2006; Kuang et al., 2006; Seale et al., 2000). Activation signals brought on by stress that is induced through muscle injury influence MuSCs to leave the quiescent state and enter the cell cycle (Feige et al., 2018).

Myogenic regulatory factors (MRFs) are involved in MuSC fate decisions. Important MRFs include the myoblast determination protein 1 (MyoD), myogenic factor 5 (Myf5), myogenin (MyoG) and myogenic regulatory factor 4 (MRF4) **(Fig. 1.1**) (Hernández-Hernández et al., 2017). Once activated, MuSCs proliferate and express both Pax7 and MyoD (**Fig. 1.1**) (Megeney et al., 1996; Zammit et al., 2006; Yablonka-Reuveni & Rivera, 1994; Smith et al., 1994). Activated MuSCs may also express Myf5 protein (**Fig. 1.1**) (Kuang et al., 2007; Relaix et al., 2005; Gayraud-Morel et al., 2012). Although most, but not all quiescent MuSCs transcribe the Myf5 gene, Myf5 mRNA is sequestered in granules and its translation is silenced by miR-31 (Crist et al., 2012).

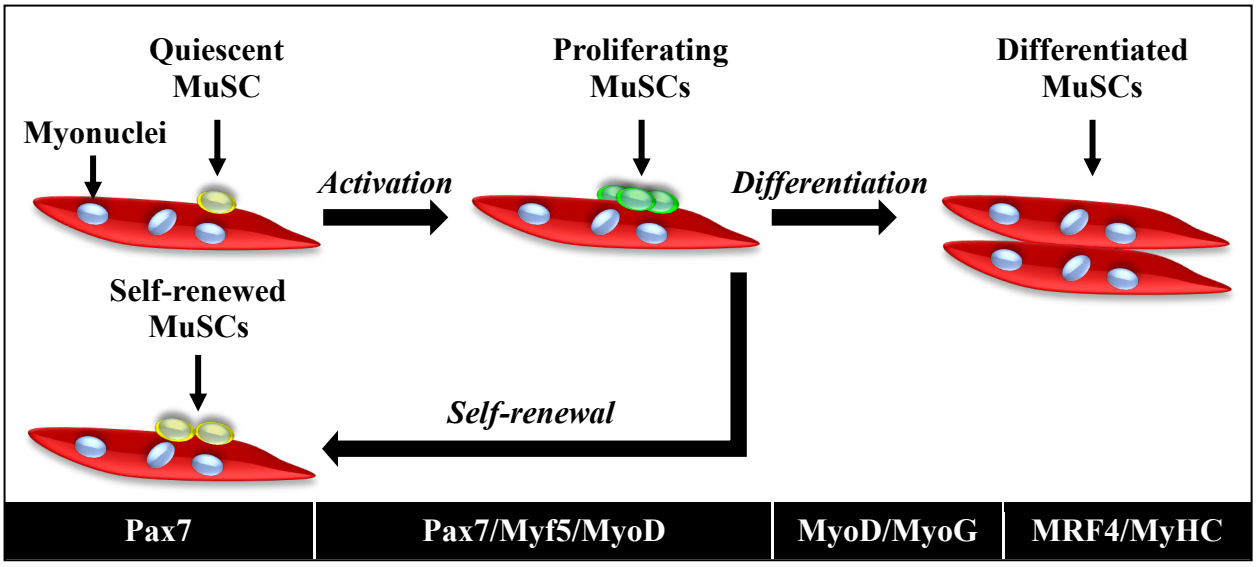

Figure 1.1. MuSC fate decisions. MuSCs reside on the periphery of myofibers in a quiescent state and are distinct from myonuclei by their expression of Pax7. After activation, MuSCs enter the cell cycle and proliferate, continuing to express Pax7, along with Myf5 and/or MyoD. Activated MuSCs will make a fate decision to either self-renew and revert to a quiescent state to replenish the MuSC pool by downregulating MyoD or commit to differentiate into muscle. During differentiation, MuSCs upregulate MyoG while downregulating Pax7, and integrate into myofibers or become new myofibers. There is an increase in MRF4 and MyHC in mature muscle.

Upon activation, these granules release Myf5 transcripts, allowing for the rapid translation into protein needed for myogenic commitment (Crist et al., 2012). Similarly, MyoD transcript has been shown to be present in quiescent MuSCs, but its translation is repressed by Staufen1 until activation (Morée et al., 2017).

MuSC proliferation is necessary for optimizing the regeneration potential of muscle. MuSCs can undergo symmetric divisions in a planar orientation parallel to the myofiber or asymmetric divisions in an apicobasal orientation perpendicular to the myofiber that are regulated by polarity proteins and mitotic spindle orientation (Dumont et al., 2015b). Symmetric divisions expand the MuSC pool by generating two identical stem cells, while asymmetric divisions maintain the population of MuSCs by generating a self-renewing MuSC and also produce a committing MuSC for muscle regeneration to occur (Wang et al. 2014). Following injury, signalling between the myofiber and MuSC with the wingless-type MMTV integration site 7A ligand and its receptor frizzled 7 leads to symmetric expansion of MuSCs through the planar cell polarity signalling pathway (Le Grand et al., 2009). This regulation of symmetric and asymmetric division is necessary to maintain optimal regenerative capacity (Dumont et al., 2015c).

MuSCs can differentiate into myocytes by upregulating MyoG while downregulating Pax7 and integrate into myofibers or become new myofibers through the process of fusion (**Fig. 1.1**) (Schmidt et al., 2019). Integration of myocytes into fibers allows for regeneration of damaged muscle. The MuSCs that do not fully commit to differentiation downregulate MyoD to revert into a quiescent state through a process known as self-renewal **(Fig. 1.1)** (Zammit et al., 2004). This process of self-renewal is vital in maintaining the stem cell pool.

To commence the differentiation program, MyoD facilitates terminal cell cycle arrest by upregulating the cyclin-dependent kinase (CDK) inhibitor p21 as well as by inducing MyoG

expression (Halevy et al., 1995; Hollenberg et al., 1993). MyoD binds to the regulatory regions of genes involved in early myogenesis and initiates histone acetylation events in late myogenesis to allow for the binding of MyoG to its target genes (Cao et al., 2006). These targets include the contractile proteins myosin heavy chain (MyHC), Troponin, Titin and Z-disc proteins (Davie et al., 2007). MyoG is necessary for effective myogenic differentiation and disruptions in the MyoG gene have resulted in perinatal lethality in mice (Hasty et al., 1993; Nabeshima et al., 1993).

1.3 Approaches to assess muscle stem cell fates

MuSC fate decisions can be tracked ex vivo using a well-established myofiber explant methodology **(Fig 1.2)** (Brun et al., 2018; Pasut et al., 2013). One of the first described protocols for myofiber isolation was by Bischoff in 1986 who demonstrated that MuSCs remain intact with the myofiber and can activate and proliferate in the presence of a mitogen rich environment (Bischoff, 1986). Interestingly, it was also shown that differentiating MuSCs on isolated myofibers do not fuse with their associated myofiber, but they will fuse to other MuSCs to form new

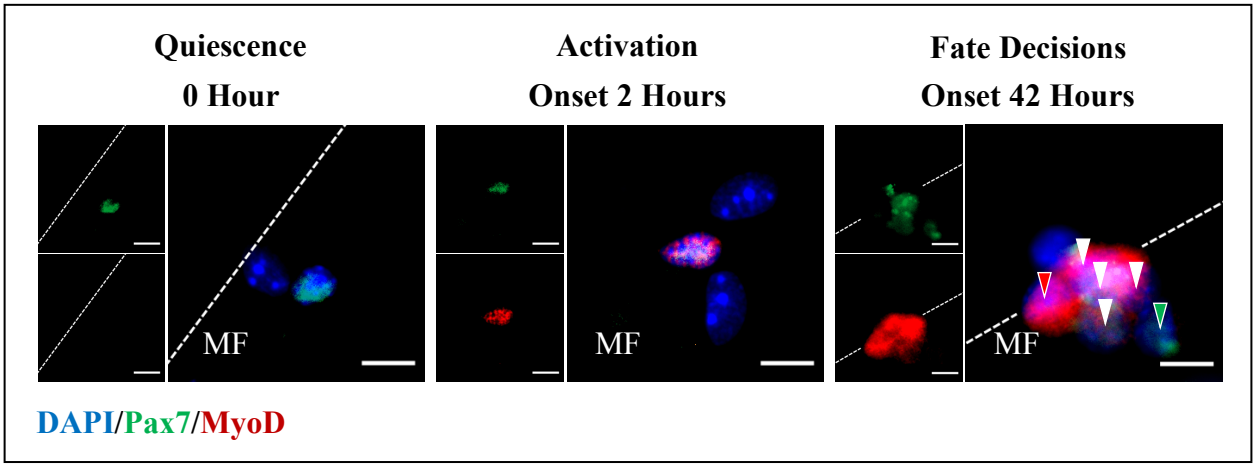

Figure 1.2. Tracking MuSC fate decisions ex vivo. MuSC fate decisions can be followed by culturing myofibers isolated from mouse extensor digitorum longus (EDL) muscle and by immunofluorescence of Pax7 (green) and MyoD (red) protein markers with nuclear marker DAPI (blue). At 0 hour in culture, MuSCs are quiescent and express Pax7 only, while activated MuSCs will express both Pax7 and MyoD. MuSCs will proliferate and form clusters of MuSCs undergoing self-renewal (green arrow), proliferation (white arrow), and differentiation (red arrow) (scale bar 10μm). Myofiber area (MF) is outlined by dashed lines.

myotubes (Bischoff, 1986). Through adaptations to this protocol, methods have developed to better understand MuSC fate decisions (Pasut et al., 2013; Hüttner et al., 2021). Freshly isolated myofibers contain quiescent MuSCs that are characterized by immunostaining for the presence of Pax7 and the absence of MyoD. Upon activation, MuSCs will express MyoD and proliferate to undergo the first division at approximately 42 hours in culture. MuSC proliferation will result in cluster formation from 72 hours in culture, with progenies of different myogenic fates. Here, Pax7 only expressing MuSCs are self-renewing, Pax7 and MyoD expressing cells are proliferating, and MyoD only cells are differentiating **(Fig 1.2)** (Pasut et al., 2013; Hüttner et al., 2021).

Myogenic progenitor cells (MPCs) or myoblasts that are cell lines such as C2C12 cells, or MuSCs that are isolated from myofibers and grown in culture, are used as in vitro cellular models to study the events involved in fate choices. As MPCs are independent of their microenvironment, they are not considered MuSCs. These cells are capable of proliferation and differentiation into myotubes in vitro **(Fig. 1.3)** (Abou-Khalil et al., 2013). A subpopulation that remains undifferentiated, quiescent and non-cycling, are termed reserve cells (RCs) **(Fig. 1.3)**. When replated, RCs can activate and differentiate into myotubes or form more RCs, thus mimicking MuSCs (Abou-Khalil et al., 2013).

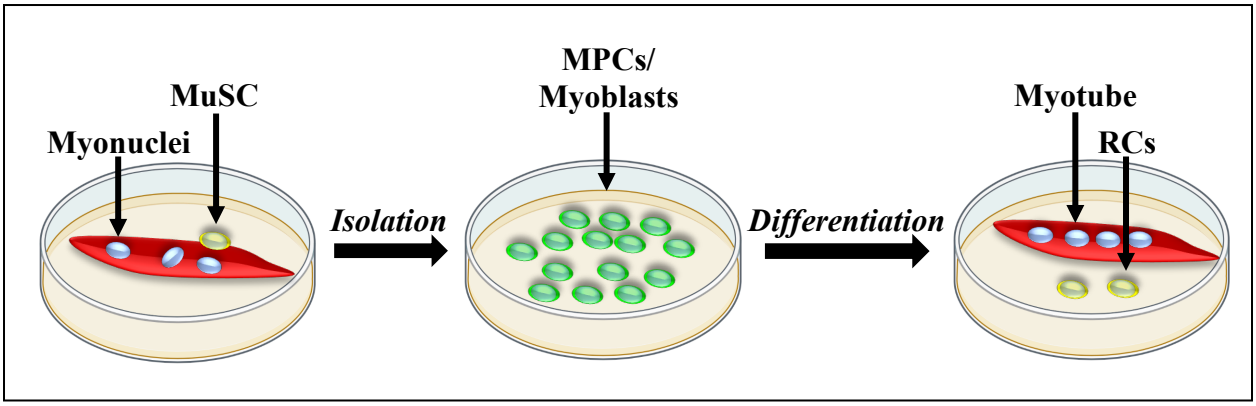

Figure 1.3. In vitro MuSC transition into myogenic progenitors or myoblasts. MuSCs that are isolated from mouse extensor digitorum longus (EDL) myofibers and cultured, are capable of differentiating into myotubes and contain a subpopulation of undifferentiated reserve cells (RCs) that can be grown and differentiated into myotubes.

1.4 Myocyte fusion

Myocyte fusion is an important step in differentiation that is controlled by tightly regulated cellular mechanisms that have been extensively studied using MPCs (Lehka & Rędowicz, 2020). As myocytes fuse into a more organized muscle architecture, appropriate myonuclear positioning is required for functionality. Nuclear movement during fusion takes place as a series of five steps that include centration, alignment, spreading, peripheral migration, and anchoring (Roman et al., 2018). During centration, the nucleus of a myocyte moves toward the centre of the myotube through the actions of the dynein/dynactin complex and microtubules that emanate from one nucleus and anchor to the nuclear envelope of another nucleus (Cadot et al., 2012). Nuclear alignment then results in the nuclei aligning on a single plane as instructed by the centrosomal and motor proteins that are recruited to the nuclear envelope via Nesprin-1 and pericentriolar material 1 (Espigat-Georger et al., 2016). Proceeding nuclear alignment is nuclear spreading in which nuclei spread across the length of the myotube (Roman et al., 2018). This is due to the microtubule-associated protein 7 linking kinesin-l to the microtubule cytoskeleton (Metzger et al., 2012). Furthermore, Nesprin-1/2 anchors kinesin-1 to distribute nuclei along the myotube (Wilson & Holzbaur, 2015). These centrally locating nuclei begin to move towards the myofiber periphery that surround the nuclei (Roman et al., 2017). Finally, nuclear anchoring is mediated by Nesprin-1 and desmin that form a flexible perinuclear scaffold to protect and cage the nuclei in its place (Chapman et al., 2014; Zhang et al., 2007; Lei et al., 2009; Wang et al., 2015).

It has been demonstrated that mitochondrial networks remodel during myocyte fusion. Prior to the third day of C2C12 differentiation when myocytes initiate fusion, there is an upregulation of dynamin-related protein 1 (DRP1) mediated mitochondrial fragmentation that decrease to undetectable levels at terminal differentiation. During myocyte fusion through day 4

of differentiation, there is an increase in the mitochondria fusion protein optic atrophy-1 (OPA1), subsequent mitochondrial biogenesis and formation of a filamentous mitochondrial network. This network remodelling is attributed to mitochondrial autophagy and turnover (Sin et al., 2016). These results suggest that mitochondrial fragmentation may be required to initiate the fusion process by eliminating existing mitochondria to make way for more robust mitochondria that provide the adenosine triphosphate (ATP) necessary for differentiation (Sin et al., 2016).

1.5 Muscle stem cell heterogeneity

The pool of quiescent MuSCs is a heterogenous population with different metabolic and functional characteristics. Heterogeneity of MuSCs can be observed through the differential expression of myogenic markers that influence MuSC fate decisions to activate, self-renew or commit to differentiate (Ancel et al., 2021). For example, the level of expression of Pax7 accounts for two subgroups of MuSCs. This was demonstrated by fluorescence activated cell sorting green fluorescent protein (GFP) expressing quiescent MuSCs from transgenic Pax7-GFP mice. The MuSCs with high levels of Pax7 ($Pax7^{High}$) had a greater lag time before the first cell division, had more stem cell markers (CXCR4 and CD34), were less primed for commitment to differentiate and had a lower metabolic rate compared to quiescent MuSCs with low levels of Pax7 ($Pax7^{Low}$) (Rocheteau et al., 2012). Furthermore, quiescent MuSCs expressing high levels of the cell surface marker CD34, had a lower metabolic rate and greater capacity for self-renewal. Conversely, quiescent MuSCs expressing low levels of CD34 were more prone to enter the cell cycle and committed to myogenesis (García-Prat et al., 2020).

Heterogeneity is also apparent based on the expression of Myf5 during MuSC development. Approximately 10% of Pax7 expressing MuSCs have never expressed Myf5 during their lifetime (Kuang et al., 2007). When activated, these Pax7+/Myf5- MuSCs can undergo

asymmetric division, producing a self-renewing $Pax7^{+}/Myf5^{-}$ and committing Pax7+/Myf5+ MuSC **(Fig. 1.4)**. Also, $Pax7^{+}/Myf5^{-}$ MuSCs can symmetrically divide, producing two copies of themselves for expansion of their populations. Furthermore, it was demonstrated that during asymmetric divisions, a majority of the cells against the basal surface are Pax7+/Myf5- and the apical cells Pax7+/Myf5+ **(Fig. 1.4)** (Kuang et al., 2007).

There also exists a heterogenous group of faster and slower dividing MuSCs that were revealed by an ex vivo study centred on the frequency of MuSC cell divisions from isolated EDL myofibers (Ono et al., 2012). The majority are fast-dividing MuSCs that give rise to a greater number of progeny, which efficiently differentiate and self-renew (Ono et al., 2012). The slow-dividing MuSCs expressed higher levels of inhibitor of deoxyribonucleic acid (DNA) binding 1, which is a known inhibitor of myogenic differentiation (Benezra et al., 1990; Sun et al., 2005; Qui et al., 2022) and retained long-term self-renewal capacity after serial passaging (Ono et al., 2012). Furthermore, transplantation of the slow-dividing cells into muscle following cardiotoxin induced damage, regenerated the muscle more efficiently and with greater engraftment potential (Ono et al., 2012).

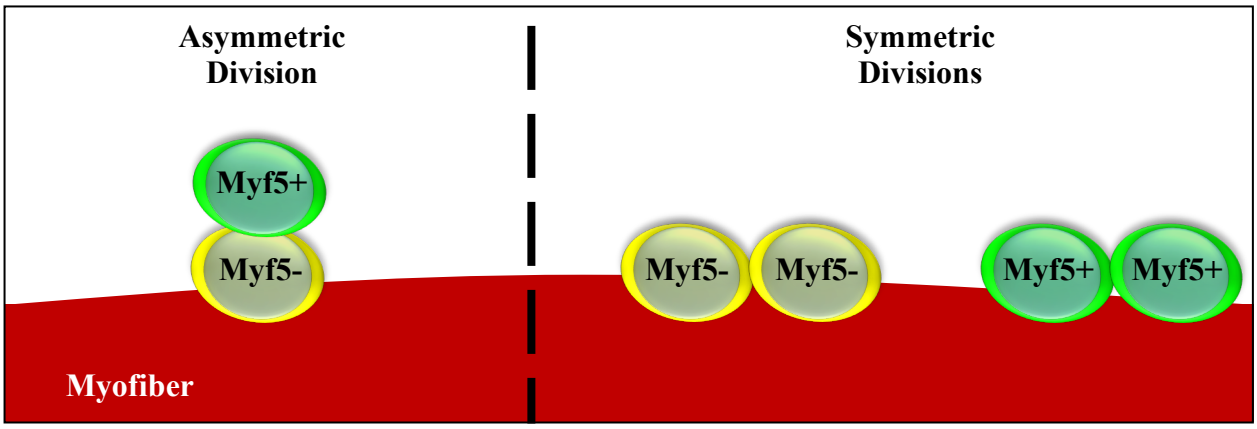

Figure 1.4. Depiction of Myf5 specific division on a myofiber. A small subset of the MuSCs found on myofibers have never expressed Myf5. These Myf5- MuSCs can asymmetrically divide to produce a committed Myf5+ MuSC and a self-renewed Myf5- MuSC. Myf5- or Myf5+ MuSCs can also symmetrically divide to expand the stem-like or committed pool of MuSCs, respectively.

Similarly, tracking MuSC proliferative history using a TetO-H2B-GFP reporter found differences in MuSC types. In this case, doxycycline induces the expression of H2B-GFP and when withdrawn, this label dilutes in proportion to cell division. The MuSCs which divide less frequently, retain the labeling (LRC) and those that divide more frequently, lose the labeling over time (nonLRC) (Chakkalakal et al., 2014). It was found that primary myoblasts isolated from mice, were comprised of an LRC subset that maintained a more primitive phenotype, as defined by a greater expression of Pax7 and a lower expression of MyoG. This LRC subset had greater transplantation potential and gave rise to nonLRCs, whereas nonLRCs were restricted to differentiate (Chakkalakal et al., 2014). Following induced injury, isolated primary myoblasts revealed that LRCs compared to nonLRCs had a lower proportion of MyoD+/Myf5+ expression after 8 hours in culture, and a greater proportion of Pax7+ expression after 4 days in culture (Chakkalakal et al., 2014).

MuSC heterogeneity can be influenced by the niche. Following injury, quiescent MuSCs from the contralateral limb of an injured muscle are phenotypically different from quiescent MuSCs in non-injured animals (Rodgers et al., 2014). It is argued that MuSCs exist and transition between a G0 and alerted phase (G^{Alert}) in response to injury-induced signals that is attributed to mammalian target of rapamycin complex 1 (mTORC1) signalling. When mTORC1 activity subsides, these G^{Alert} MuSCs revert back to MuSCs with G0 properties (Rodgers et al., 2014). The MuSCs in a G^{Alert} state have a quickened response to enter the cell cycle following mitogenic stimuli, enhanced differentiation kinetics and cell fusion compared to MuSCs in a G0 state. Interestingly, genes involved in mitochondrial metabolism are strongly correlated to this transition to G^{Alert} suggesting that the mitochondria are important players in stem cell quiescence (Rodgers et al., 2014).

1.6 Mitochondria

Mitochondria are highly dynamic organelles that play a vital role in many cellular processes including the regulation of energy production, biosynthetic precursor balance, cytosolic calcium levels, redox status, apoptosis, and the generation of reactive oxygen species (ROS) (Abate et al., 2020). Structurally, mitochondria are double membrane organelles consisting of an inner mitochondrial membrane (IMM) and outer mitochondrial membrane (OMM) **(Fig. 1.5)** (Pfanner et al., 2019). The IMM and OMM separates the mitochondria into two compartments, the first being the intermembrane space (IMS) between the IMM and OMM, and the other being the matrix within the IMM (Abate et al., 2020). The IMM contains invaginations called cristae, which allows for greater surface area (Pfanner et al., 2019).

The mitochondria are not individual stationary organelles but rather, are highly networked and motile, while responsive to cellular metabolism (Fenton et al., 2021; Rahman & Quadrilatero, 2021). The networking of mitochondria acts to distribute information over distances and provides a method for communication between mitochondria. For example, it was found that the mitochondrial network acts as a conductive path for energy distribution in the form of the proton motive force (PMF), throughout skeletal muscle (Glancy et al., 2015). Furthermore, networked mitochondria can recognize local dysfunction by sensing changes in the mitochondrial potential energy and act within seconds to limit its spread through their intermitochondrial junctions (Glancy et al., 2017). This characteristic of mitochondria gives importance to its structure for proper cell functioning.

Mitochondria house their own DNA (mtDNA) that replicate in conjunction with mitochondrial fission **(Fig. 1.5)** (Ban-Ishihara et al., 2013). Located in the mitochondrial matrix, mtDNA is packaged into nucleoprotein complexes known as nucleoids (Nicholls et al., 2018).

mtDNA is a closed circle double-stranded DNA that in humans consist of 16,569 base pairs that encode 13 proteins that are subunits of four of the five electron transport chain (ETC) complexes, 22 transfer ribonucleic acids and 2 ribosomal ribonucleic acids required to synthesize these proteins (Nicholls et al., 2018).

Mitochondria are the central hubs for converting glucose, free fatty acids (FFAs) and amino acids into usable energy in the form of ATP while also producing metabolites involved in cell

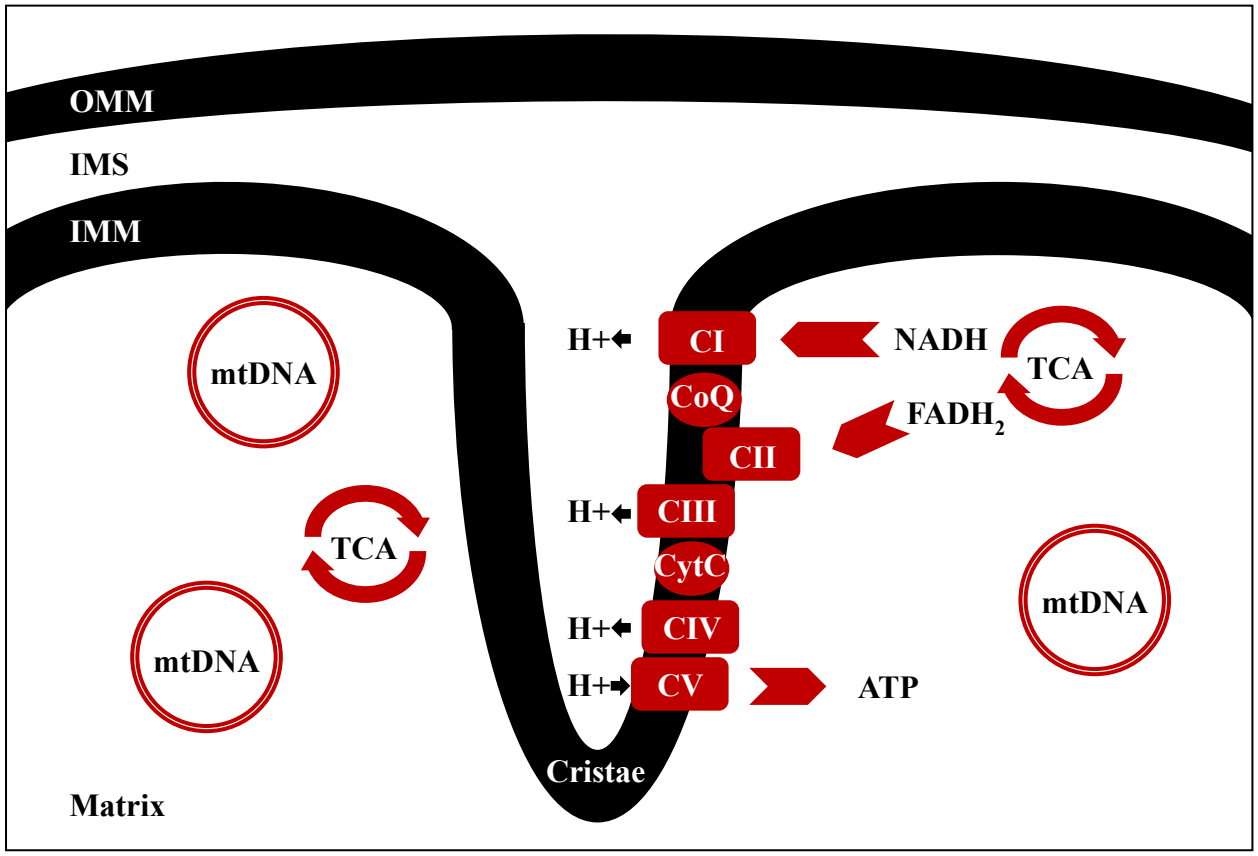

Figure 1.5. Diagram of mitochondrial structure and components. The architecture of the mitochondria consists of the outer mitochondrial membrane (OMM), intermembrane space (IMS), inner mitochondrial membrane (IMM) and matrix. Invaginations called cristae, house the electron transport chain (ETC) and their complexes. Reduced nicotinamide adenine dinucleotide (NADH) and reduced flavin adenine dinucleotide ($FADH_2$) substrates produced by the tricarboxylic acid (TCA) cycle are oxidized and electrons shuttled across the ETC complexes (C) I-V, ubiquinone (CoQ) and cytochrome c (CytC). In the process, a proton motive force (PMF) is generated by proton movement into the IMS which provides the energy to synthesize ATP. The mitochondrial DNA (mtDNA) is located in the matrix and encodes proteins for the ETC.

signaling (Martínez-Reyes & Chandel, 2020). In the mitochondrial matrix, the tricarboxylic acid (TCA) cycle produces reduced nicotinamide adenine dinucleotide (NADH) and reduced flavin adenine dinucleotide ($FADH_2$) through a series of enzymatic reactions. NADH and FADH produced from these systems, can donate their electrons to the ETC that contains the complexes necessary for oxidative phosphorylation (OXPHOS) to produce ATP (Martínez-Reyes & Chandel, 2020). An important substrate that feeds into the TCA cycle is acetyl-CoA derived from FFAs, amino acids, or pyruvate oxidation (Martínez-Reyes & Chandel, 2020). The FFAs can be shuttled into the mitochondria through FFA transport systems and undergo beta-oxidation to produce acetyl-CoA (Knottnerus et al., 2018). Central to the generation of pyruvate is glycolysis which takes place in the cytoplasm through the conversion of glucose (Lunt & Vander Heiden, 2011). In the absence of oxygen or when the TCA cycle/ETC is saturated, pyruvate produced from glycolysis converts into lactate instead of acetyl-CoA (Lunt & Vander Heiden, 2011). Thus, the relative contributions from glycolysis and OXPHOS depends on the ATP requirements and substrate availability.

The ETC is made up the mobile electron carriers ubiquinone (CoQ) and cytochrome c (CytC) and complexes I to V, with each successive electron acceptor complex being a more potent electron acceptor than the previous **(Fig. 1.5)** (Cadonic et al., 2016). The synthesis of ATP through OXPHOS occurs as a stepwise process of electron transfer through the ETC complexes and subsequent proton movement from the matrix into the IMS generating an electro-chemical potential gradient and PMF. The IMS protons then pass through F0/F1-ATP synthase to generate ATP from adenosine diphosphate (ADP) **(Fig. 1.5)** (Van Der Bliek et al., 2017; Mitchell, 1961).

Electron transport is directly coupled to proton translocation and therefore, the rate of electron flow depends on the magnitude of the PMF (Berry et al., 2018). When there is a reduced

electron flow rate because of an elevated PMF, there is backpressure on the ETC proton pumps which can cause electron leakage and the production of reactive oxygen species (ROS) primarily at CI and CIII (Wong et al., 2017). The production of ROS occurs when free electrons react with oxygen to produce superoxide. The mitochondria specific antioxidant, superoxide dismutase, converts superoxide into hydrogen peroxide and glutathione peroxidase then converts hydrogen peroxide into water. Without the action of glutathione peroxidase, hydrogen peroxide can become a highly reactive hydroxyl radical (Oyewole & Birch-Machin, 2015). Although elevated ROS levels are associated with various disease states (Brieger et al., 2012), ROS can also act as signaling molecules in apoptosis, autophagy, hypoxia, innate immunity, endoplasmic reticulum stress and stem cell fates (Lim et al., 2015; Li et al., 2013; Chandel et al., 2000; West et al., 2011; Win et al., 2014; Tormos et al., 2011).

1.7 Mitochondria and muscle stem cells

Mitochondria are implicated in MuSC functioning that include fate decisions (Bhattacharya & Scimè, 2020). Mitochondrial metabolic profile changes throughout MuSC fate decisions, where MuSCs rely primarily on OXPHOS in quiescence and terminal differentiation, and glycolysis during activation and proliferation (Bhattacharya & Scimè, 2020) **(Fig. 1.6)**. Quiescent MuSCs have a greater reliance on mitochondrial FFA oxidation for ATP production and a lower reliance on glycolysis (Ryall et al., 2015). MuSCs in a deep quiescent state display reduced metabolism, consume less oxygen, produce lower levels of ATP, have a reduced mitochondrial mass, reduced transcription of mitochondrial genes, and increased mtDNA content (Latil et al., 2012). Following activation, quiescent MuSC undergo a metabolic shift from relying primarily on the mitochondria for FFA oxidation, towards glycolysis (Ryall et al., 2015; Bhattacharya & Scimè, 2020). This change in metabolism is necessary to sustain the anabolic demands of proliferating

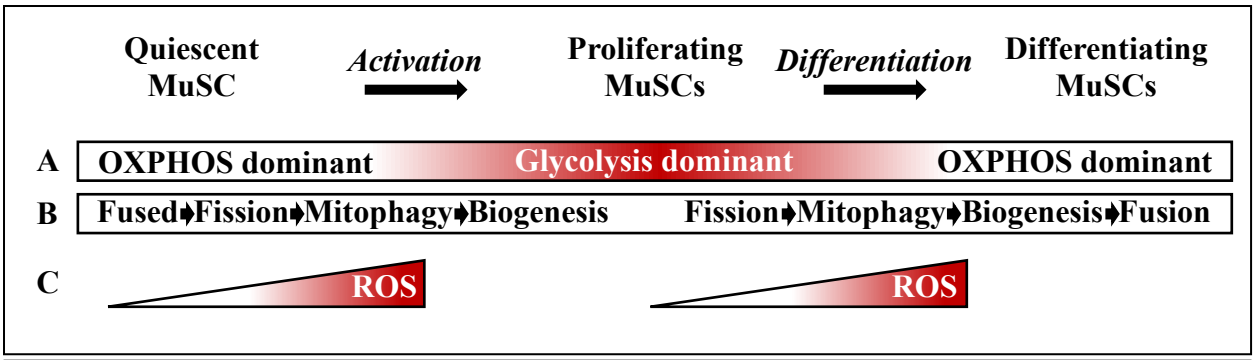

Figure 1.6. Diagram of the metabolic shift and mitochondrial alterations during fate decisions. **A:** The dominant metabolic system during MuSC quiescence is OXPHOS, which shifts towards a more glycolytic state upon activation. During differentiation, there is less reliance on glycolysis in favour of OXPHOS. **B:** The mitochondrial network is remodelled throughout fate decisions. Quiescent MuSCs undergo fission upon an activation stimulus to remodel the mitochondria for proliferation. This is also the case in the transition from proliferation to differentiation. **C:** The levels of ROS increase during activation and differentiation, subsequent to mitochondrial fission.

MuSCs. Here there is a greater production of the macromolecules needed to support anabolic requirements and a redirection away from OXPHOS towards extracting substrates from the TCA cycle (Folmes et al., 2012). Interestingly, MuSCs that display increased commitment at the expense of self-renewal have a decrease in TCA cycle, OXPHOS and lipid metabolism, with an upregulation in glycolysis related genes (Pala et al., 2018).

During the differentiation process, OXPHOS is favoured over glycolysis (Bhattacharya & Scimè, 2020). As differentiation progresses, there is a steady increase in enzymes for oxidative metabolism, ETC complex proteins, mtDNA content and mitochondrial biogenesis regulators (Remels et al., 2010; Hoffmann et al., 2018; Sin et al., 2016). The importance of OXPHOS is shown when shifting metabolism away from OXPHOS, by deleting pyruvate dehydrogenase, the enzyme involved in producing acetyl-CoA from pyruvate, resulted in inefficient skeletal muscle regeneration, terminal differentiation and myotube formation (Hori et al., 2019).

The increase in oxidative metabolism during differentiation can be attributed to MyoD acting as an upstream regulator of mitochondrial biogenesis proteins (Shintaku et al., 2016).

Silencing of MyoD reduced TCA cycle activity and FFA oxidation (Shintaku et al., 2016). The mitochondrial activity necessary for differentiation also operates to enhance MRF function. When mitochondrial protein translation is inhibited by chloramphenicol treatment, there is an associated inhibition of myoblast differentiation. This comes not as a result of reduced ATP production, but by influencing the expression of MyoG (Rochard et al., 2000; Seyer et al., 2006; Seyer et al., 2011).

To address the increase in metabolic demand of differentiating myotubes, a change in metabolism from glycolysis to OXPHOS requires remodelling of the mitochondrial network **(Fig. 1.6)**. In the early stages of myogenic differentiation, there is increased DRP1 activity that causes mitochondrial fragmentation and mitophagy (Sin et al., 2016; Kim et al., 2013). This brief period of fission and mitochondrial clearance is followed by increased mitochondrial biogenesis. Here, OPA1 is upregulated to reform mitochondrial networks which are better primed for OXPHOS (Sin et al., 2016). The fission event that occurs prior to fusion is necessary for differentiation, as blocking autophagy impairs myogenic differentiation (Sin et al., 2016). Furthermore, inhibition of DRP1 results in reduced mitochondrial biogenesis and mtDNA content (Kim et al., 2013). Interestingly, enhanced DRP1 and fragmentation delayed myogenic differentiation, suggesting that there is a tight regulation of fission/fusion dynamics for myogenic differentiation and that mitochondrial elongation is necessary for differentiation (De Palma et al., 2010). Mitochondrial fission is also implicated in the transition between quiescence and proliferation of MuSCs during regeneration (Hong et al., 2022). Here, mitochondrial fission allows for quiescence exit and MuSC expansion by permitting mitophagy and OXPHOS metabolic reprogramming (Hong et al., 2022).

1.8 Reactive oxygen species and differentiation

An essential signalling molecule for differentiation is mitochondrial ROS, which increases during myogenic differentiation **(Fig. 1.6)** (Malinska et al., 2012). The paired-like homeodomain transcription factors 2 and 3 (Pitx2 and Pitx3) have been found to regulate ROS levels during myogenic differentiation (L'honoré et al., 2014). Genetic deletion of Pitx2 and Pitx3 causes the accumulation of abnormally high levels of ROS in differentiating myoblasts by downregulating nuclear respiratory factor 1, resulting in DNA damage and apoptosis (L'honoré et al., 2014). However, moderate overproduction of ROS through single Pitx3 mutants, results in premature MuSC differentiation through phosphorylation of p38α which induces the expression of MyoG. Furthermore, when these MuSCs are treated with the ROS scavenger N-acetyl-cysteine or a p38α inhibitor, myogenic differentiation is prevented (L'honoré et al., 2018). These results suggest that MuSCs are highly sensitive to ROS fluctuations and that increased ROS facilitates MuSC differentiation.

Mitochondrial fragmentation is linked to stem cell fate decisions through a ROS mediated pathway. Mitochondrial fragmentation is associated with increased ROS levels in myotubes (Yu et al., 2006; Jheng et al., 2012), which may be the pathway involved for inducing myogenic differentiation. Mitochondrial fragmentation in neural stem cells has been shown to increase ROS levels, which upregulates nuclear factor erythroid 2-related factor 2, where it will bind to nuclear DNA to suppress self-renewal genes and promote differentiation (Khacho et al., 2016).

1.9 Retinoblastoma-like protein 2

The retinoblastoma susceptibility (Rb) gene family members are implicated in mammalian cell cycle regulation and consist of the retinoblastoma associated protein 1 (Rb1), retinoblastoma-like protein 1 (Rbl1) and retinoblastoma-like protein 2 (Rbl2) (Fischer & Müller, 2017; Henley &

Dick, 2012). They have well-defined roles as nuclear co-repressors, where they do not bind directly to DNA but to the E2F transcription factors (Cobrinik, 2005). When an Rb protein is bound to an E2F transcription factor, they recruit chromatin remodeling enzymes that repress the genes needed for cell cycle progression (Frolov & Dyson, 2004). CDKs are responsible for phosphorylating Rb proteins, which allows for the dissociation of E2F from its target genes **(Fig. 1.7)** (Łukasik et al., 2021). Despite the structural similarities between the Rb family members (Classon & Dyson, 2001), some important differences exist. Rb1 is the only protein that interacts with E2F1-3, whereas Rbl2 and Rbl1 only bind to E2F4 and E2F5 (Liban et al., 2016; Liban et al., 2017). Furthermore, Rbl2 and Rbl1 have a higher sequence similarity between each other than with Rb1 (Classon & Dyson, 2001). The nuclear expression of Rb proteins also vary in different cell states, where Rb1 is expressed during quiescence, proliferation and differentiation, and typically, Rbl1 during proliferation and Rbl2 in quiescence and differentiation (Flores & Goodrich, 2022).

Recently, there have been documented cases of human Rbl2 mutations in the literature (Brunet et al., 2020; Samara et al., 2021). Individuals with this mutation present with severe developmental delays, muscle hypotonia and most are wheelchair bound (Brunet et al., 2020;

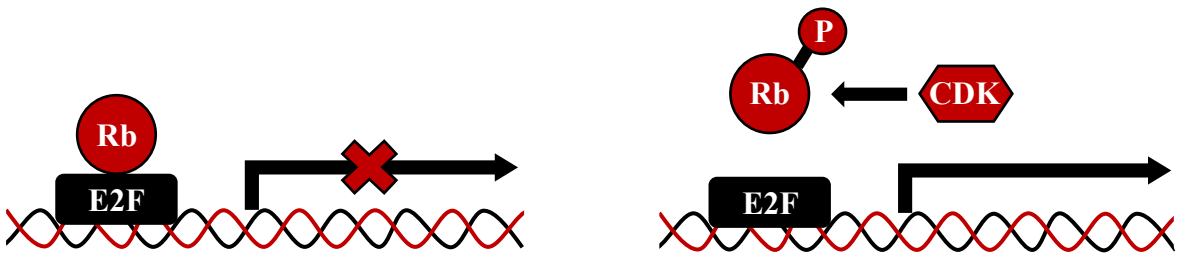

Figure 1.7. Schematic demonstrating the nuclear function of the retinoblastoma susceptibility (Rb) gene family. The Rb proteins bind to the E2F transcription factors to repress transcriptional activity. Upon phosphorylation by the cyclin-dependent kinases (CDKs), binding to E2F is abrogated which allows gene transcription to ensue.

Samara et al., 2021). It has also been demonstrated that mice of Balb/cJ genetic background with a Rbl2 null mutation die between embryonic days 11 and 13, display severe impairments in neurogenesis and myogenesis, and exhibit increased apoptosis (LeCouter et al., 1998). Interestingly, mice with a mixed 129/Sv:C57BL/6J genetic background are viable, suggesting that Rbl2 plays a role in a strain-dependent manner during development (Cobrinik et al., 1996). In C2C12 myoblasts, Rbl2 is expressed at low levels and is present in RCs (Carnac et al., 2000). Forced overexpression of Rbl2 in C2C12 myoblasts inhibited proliferation, but when supplemented with differentiation medium, the cells express low levels of MyoG suggesting that Rbl2 overexpression may inhibit differentiation. Overexpression of Rbl2 was also found to inhibit MyoD expression and protein activity, which may be part of the pathway that maintains RCs (Carnac et al., 2000). Thus, Rbl2 may have MuSC fate decision specific functions.

CHAPTER 2

RATIONALE, HYPOTHESIS AND OBJECTIVES

Rationale

There has been a growing body of evidence of a metabolic role for the Rb family members in stem cells. It has been shown that preadipocyte differentiation into white or brown fat is regulated through the actions of Rb1 and Rbl1 by influencing peroxisome proliferator-activated receptor gamma coactivator 1-alpha expression and metabolic reprogramming (Scimè et al., 2005; De Sousa et al., 2014; Porras et al., 2017). Knockdown of Rbl1 also increases the thermogenic and oxidative capacity of differentiating mesenchymal stem cells (De Sousa et al., 2014). Furthermore, there is evidence of a downstream Rbl1 regulatory pathway involving mitochondria and the proliferative fate of MPCs (Bhattacharya et al., 2021). In this regard, Rbl1 translocates to the mitochondrial matrix under conditions of low cytoplasmic nicotinamide adenine dinucleotide (NAD^+)/NADH, where it interacts at the mitochondrial DNA to repress transcription of mitochondrial genes, resulting in reduced OXPHOS and proliferation (Bhattacharya et al., 2021).

Thus, given the structural and functional similarities Rbl2 has with Rbl1, and the adverse effect on skeletal muscle that the Rbl2 mutation and genetic deletion cause in humans and mice respectively, Rbl2 was investigated during MuSC fate decisions. The comprehensive characterization of Rbl2 in MuSC fate decisions before this thesis had yet to be conducted.

Hypothesis

Rbl2 is localized in the mitochondria during MuSC fate decisions.

Objectives

The goal of this research project is to characterize Rbl2 in MuSC fate decisions using 3 specific aims.

Aim 1: To identify if Rbl2 promotes muscle differentiation

Aim 2: To identify if Rbl2 protein is expressed during MuSC fate decisions

Aim 3: To ascertain the cellular localization of Rbl2 protein during MuSC differentiation

CHAPTER 3

MATERIAL AND METHODS

Mice

Experiments involving the use of animals were conducted in accordance with the guidelines set by the Animal Care Committee of York University, which are based on the guidelines of the Canadian Council on Animal Care. Wildtype (WT) mice of background NMRI, C57/B16, FVB/N were used for all animal experiments (Bhattacharya et al*.,* 2021). The mice were aged 6 to 8 weeks.

Cell line

C2C12 cells are an immortalized mouse myoblast cell line derived from C3H mouse leg and were purchased from the American Type Culture Collection. The cells were cultured in 10-cm tissue culture dishes containing Dulbecco's Modified Eagle Medium (DMEM) (Wisent Bioproducts) with 25mM glucose, supplemented with 10% fetal bovine serum (FBS) (Wisent Bioproducts) and 1% penicillin streptomycin (P/S) (Wisent Bioproducts) at 37°C with 5% CO2. For differentiation experiments, C2C12 cells were grown to confluency and growth arrested (GA) in 10-cm tissue culture dishes before adding differentiation media containing 25mM glucose DMEM, 2% horse serum (Wisent Bioproducts) and 1% P/S at 37°C with 5% CO2, for the period of time described in the results section.

Rbl2KO and Ctl cell line derivation

Genetically deleted Rbl2 (Rbl2KO) and control (Ctl) C2C12 cell lines were generated using CRISPR/Cas9. These cells served as a control to test the Rbl2 antibody to confirm its specificity for western blotting and immunofluorescence. The Rbl2KO cells were transfected with 3 pLenti-U6-sgRNA-SFFV-Cas9-2A-Puro plasmids each containing a different single guide ribonucleic acid (sgRNA) to target Rbl2 sequences 113 CGAGCCATCAGATCCAGCAG, 153 CCGCCTCAACATGGACGAGG and 204 TGTAGCTCTCGCTCATGCTG (Applied Biological Materials). The Ctl cells were transfected with an empty vector pLenti-U6-sgRNA-SFFV-Cas9-2A-Puro with scrambled sgRNA (Applied Biological Materials). For cell transfections, 10μg of each plasmid, 2.5M $CaCl_2$, and double distilled water (ddH_2O), for a total volume of 500μL, was pipetted dropwise into a tube containing 500μL of HEBS buffer pH 7.05 (274mM NaCl, 10mM KCl, 1.4mM Na_2HPO_4, 15mM D-glucose, and 42mM HEPES) while gently vortexing. This 1ml mixture was incubated at room temperature for 1 hour and then added dropwise to C2C12 cells that were grown on 10-cm tissue culture plates in culturing media at 30% confluence. After 18 hours of exposure to transfection media, the cells were washed with phosphate buffered saline (PBS: 3.8mM NaH_2PO_4, 16.2mM Na_2HPO_4, and 149mM NaCl) and refed with culturing media. After 6 hours, cells were passaged onto 96-well tissue culture plates. For clonal selection, 3mg/ml of puromycin was added the next day and for every 2 days following, for a total of 3 times. Selected cells were passaged up to 10-cm cm tissue culture dishes for expansion. To test for the presence or absence of Rbl2 protein, cells were grown to confluency and GA in 10-cm tissue culture dishes, then western blotted.

Whole cell protein isolation

C2C12 cells were washed twice with PBS and scraped in radioimmunoprecipitation assay buffer (0.5% NP-40, 0.1% sodium deoxycholate, 150mM NaCl, 50mM Tris-Cl pH 7.5, 5mM EDTA) containing 1 mg/ml of pepstatin, leupeptin and aprotinin protease inhibitors and then placed on ice for 10 minutes. The lysate was then centrifuged at 21000g for 15 minutes at 4°C to remove cellular debris, and the supernatant was collected.

Mitochondrial and cytoplasmic protein isolation

C2C12 cells were washed twice, scraped in ice cold PBS and centrifuged at 1500rpm for 5 minutes. The pellet was dissolved in 150µl of mitochondrial buffer pH 7.4 (0.25mM sucrose, 0.1% BSA, 0.2mM EDTA, and 10mM HEPES, with 1 mg/ml of each protease inhibitor, pepstatin, leupeptin and aprotinin). Cells were homogenized using a prechilled Dounce homogenizer, with a loose rod (6 times) followed by a tight rod (6 times). The homogenate was then centrifuged at 1000g at 4°C for 10 minutes and the supernatant was transferred to a new tube. The supernatant was then centrifuged at 14000g for 15 minutes at 4°C to separate cytosolic (supernatant) and mitochondrial (pellet) fractions. Once separated, the supernatant was transferred to a new tube while the pellet was resuspended in 120µl of mitochondrial buffer. To ensure purity, the pellet was washed 3 times. On the final wash, the pellet was resuspended in 30µl of mitochondrial buffer. The mitochondria were lysed by freezing and thawing on dry ice three times.

Western blot analysis

Whole cell, cytosolic, or mitochondrial lysates were denatured in loading buffer (4% SDS, 10% 2-mercaptoethanol, 20% glycerol, 0.004% bromophenol blue, 0.125M Tris-HCl and 1mM

DTT) for 3 minutes at 100°C. These were loaded onto 8% or 10% polyacrylamide gels in 1X running buffer (90% ddH_2O and 10% of 10X running buffer containing 25 mM Tris-base, 192 mM glycine and 0.1% SDS). Proteins were separated by electrophoresis at 30mA for 90 minutes and then transferred to a 0.22μm pore sized nitrocellulose membrane (Santa Cruz Biotechnology) at 4°C at 100V for 80 minutes in transfer buffer (50mM Tris-base, 384mM glycine, 20% methanol). The membranes were then blocked at room temperature for one hour in 5% non-fat milk diluted in Tris-buffered saline (TBS: 50mM Tris-base and 150mM NaCl) with 0.1% Triton X-100 (TBST) and then washed for 5 minutes in TBST. Membranes were probed with primary antibody diluted 1:2000 for Rbl2, 1:1500 for Cox4, 1:5000 for α-Tubulin in TBST with 1% BSA at 4°C overnight with gentle rocking. The next day, membranes were washed with TBST three times for 5 minutes and then secondary antibodies diluted 1:5000 in 5% non-fat milk in TBST, were added for 1 hour at room temperature with gentle rocking. TBST was used to wash membranes three times for 5 minutes with a final wash with TBS for 10 minutes. The membranes were visualized with chemiluminescence Clarity Western ECL Substrate (Bio-Rad Laboratories) on photographic UltraCruz Nitrocellulose Pure Transfer film (Santa Cruz Biotechnology). Western blot experiments have been performed at least three independent times with similar results.

Primary myofiber isolation

Extensor digitorum longus (EDL) muscles were dissected tendon to tendon from mice and digested in filtered sterilized 0.2% type 1 collagenase (Sigma Aldrich) and 25mM glucose serum free DMEM for 1 hour at 37°C. After fibers unraveled, contents were transferred to a pre-warmed 6-cm tissue culture dish containing 25mM glucose serum free DMEM and 1% P/S. The muscles were mechanically flushed with the media using a bore pipette to induce the release of single

myofibers. Single fibers were transferred to a 24-well tissue culture plate with pre-warmed fiber culture media containing 25mM glucose DMEM, 20% FBS, 1% P/S, 1% chick embryo extract (MP Biomedicals) and 7.5 ng/mL basic fibroblast growth factor (PeproTech) and cultured for various times specified in the results section. For MuSC differentiation experiments, the fibers were cultured for 72 hours and then transferred to differentiation media containing 25mM glucose DMEM, 5% horse serum and 1% P/S for the period of time specified in the results section.

Primary myogenic progenitor cell (pMPC) isolation

For pMPC isolation, 72 hour cultured fibers were washed with PBS and transferred to rat tail collagen I (ThermoFisher Scientific) coated Nunc LabTek™ II chambered tissue culture plates (ThermoFisher Scientific) containing fiber culture media. After 2 days, wells were washed with PBS. For differentiation, GA pMPCs were provided with differentiation media containing 25mM glucose DMEM, 5% horse serum and 1% P/S for the period of time specified in the results section.

Immunocytochemistry

Before fixation, pMPCs were washed twice with PBS, and incubated in serum free 25mM glucose media containing 100nM MitoTracker™ Deep Red FM (Invitrogen) in the dark for 15 minutes at 37°C and 5% CO2. After incubation, cells were washed 3 times with PBS and fixed for 10 minutes in 4% paraformaldehyde (PFA). C2C12 cells were washed twice with PBS and fixed for 10 minutes in 90% ice-cold methanol. PFA or methanol fixed cells were washed twice with PBS and blocked for 1 hour at room temperature using blocking solution (0.3% Triton X-100, 5% donkey serum, 5% goat serum, and 3% BSA in PBS). Blocking solution was removed and cells were washed twice with wash buffer (5% Triton X-100 in PBS) for 5 minutes. The cells were then

incubated with primary antibody in blocking solution at a 1:100 dilution at room temperature for 1 hour. Primary antibody was removed and cells were washed twice with wash buffer for 5 minutes. The cells were then incubated with secondary antibody in blocking solution at a 1:200 dilution for 1 hour. Secondary antibody was removed and cells were washed twice with wash buffer for 5 minutes. The cells were then stained with 4′,6-diamidino-2 phenylindole (DAPI) for 5 minutes at a 1:10,000 dilution in PBS and then washed twice with PBS for 5 minutes. Cover slips were mounted with Vectashield mounting media (Vector Laboratories). Confocal images were taken using the Axio Observer.Z1 microscope (Zeiss) with alpha Plan-Apochromat 63x/Oil DIC (UV) M27 (Zeiss). Digital images were taken using the Axiocam MR R3 and the Axio Scope.A1 (Zeiss) using the EC Plan-Neofluar 20x/0.5 (Zeiss).

For visualizing myofiber associated MuSCs, isolated myofibers were transferred to a 24-well plate coated with FBS and fixed in prewarmed 2% PFA for 10 minutes while rocking at room temperature. The fibers were then washed 3 times with PBS and permeabilized using permeabilization solution (0.3% Triton X-100, 0.1M Glycine in PBS) for 10 minutes while rocking at room temperature. Fibers were then blocked in fiber blocking solution (5% donkey serum, 5% goat serum, 2% BSA, 0.1% Triton X-100 in PBS) for 1 hour at room temperature while rocking. After blocking, myofibers were incubated with primary antibody in fiber blocking solution at a 1:100 dilution while rocking at 4°C overnight. The next day, myofibers were washed three times with PBS for 5 minutes. The fibers were then incubated with secondary antibody in fiber blocking solution at a 1:1000 dilution for 1 hour at room temperature. The fibers were washed 3 times with PBS for 5 minutes and then stained with DAPI for five minutes at a 1:1000 dilution in PBS and then washed two more times with PBS. Fibers were transferred to positively charged microscope slides (FroggaBio) and cover slips were mounted with Vectashield mounting media (Vector

Laboratories). Digital images were taken using the Axiocam MR R3 and the Axio Scope.A1 using the EC Plan-Neofluar 40x/0.75 (Zeiss). A minimum of 10 myofibers with 15 fields of view were imaged per timepoint from each mouse. For quantification of MyoD+ MuSCs expressing/non-expressing Rbl2, Rbl2+MyoD+ or Rbl2-MyoD+ MuSCs were added and expressed as a percentage of total MyoD+ MuSCs. For quantification of the cellular location of Rbl2 protein during differentiation, Rbl2+MyoG+ MuSCs that had Rbl2 localized to the nucleus were added and expressed as a percentage of total Rbl2+ MyoG+ MuSCs.

Myofusion & differentiation index

The Rbl2KO and Ctl MPCs were differentiated for 5 days and stained with DAPI and for MyHC. Myofusion index or differentiation potential was then calculated as the fraction of the number of positive nuclei (DAPI expressing) inside myotubes (defined by MyHC expression), divided by the total number of myotubes expressing MyHC. Data was expressed as fold change between Ctl and Rbl2KO. Differentiation index, which measures the ability of MPCs to differentiate, was determined as the fraction of the number of nuclei inside myotubes, divided by the total number of nuclei in the field of view and expressed as a percentage. Both myofusion index and differentiation index were assessed with at least 6 independent fields of view of 6 Rbl2KO and 4 Ctl MPC samples.

Femoral artery ligation-induced muscle regeneration

Muscle ischemia was induced in mice aged 8-10 weeks, by unilateral ligation of the femoral artery. This method blocks the blood flow to one hindlimb while allowing the other to act as a control. Laser Doppler blood perfusion imaging using the PeriScan PIM 3 System (Perimed)

was used to confirm that blood flow was occluded. Blood flow was imaged pre, post-ligation and before mouse sacrifice. Ligation surgeries were conducted by George Nader. The tibialis anterior (TA) muscle was extracted after 4 days of ligation and fixed in 4% PFA for 1 hour. This was followed by sucrose infiltration where the TA was submerged in PBS with 15% sucrose for 1 hour, and then PBS with 30% sucrose overnight. After fixation, the muscle was imbedded in optimal cutting temperature compound (ThermoFisher Scientific) and frozen in liquid nitrogen-cooled isopentane. Following TA freezing, longitudinal sections were cut at 20μm thickness using a cryostat onto positively charged microscope slides (ThermoFisher Scientific) for immunohistochemistry. Sections were prepared and cut by Mark Danesh.

Immunohistochemistry of muscle cross sections

Longitudinal sections were washed with PBS and fixed with 4% PFA for 15 minutes at room temperature, followed by two additional washes with PBS to remove excess PFA. Sections were then blocked with blocking buffer (5% goat serum, 5% donkey serum, 0.1% Triton X-100 in PBS) for 30 minutes followed by two washes with PBS. Sections were then incubated with primary antibody in blocking buffer at a 1:100 dilution for 1 hour at room temperature. The sections were washed three times in wash buffer (5% Triton X-100 in PBS) for 5 minutes each. The sections were then incubated with secondary antibody in blocking buffer at a 1:200 dilution for 1 hour at room temperature. Secondary antibody was removed and the tissue was washed three times in wash buffer for 5 minutes. The sections were then stained with DAPI for 10 minutes at a 1:10,000 dilution in PBS and washed twice in wash buffer. Cover slips were mounted with Vectashield mounting media (Vector Laboratories). Confocal images were taken using the Axio Observer.Z1 microscope with alpha Plan-Apochromat 63x/Oil DIC (UV) M27 (Zeiss).

Antibodies

Primary antibodies for western blotting: α-Tubulin (66031-1-Ig, Proteintech); Cox4 (ab16056, Abcam); Rbl2 (RBL2-D9T7M, Cell Signalling). Secondary antibodies for western blotting: Goat anti-rabbit IgG (H+L) HRP Conjugate (170-6515, BioRad); Goat Anti-Mouse IgG (H+L) HRP Conjugate (170-6516, BioRad). Primary antibodies for C2C12 immunocytochemistry: MyHC (sc-376157, Santa Cruz Biotech). Secondary antibodies for C2C12 immunocytochemistry: Donkey Anti-Mouse IgG Secondary Antibody NL 493 conjugated (NL009, Novus Biologicals). Primary antibodies for fiber and pMPC immunocytochemistry: Rbl2 (sc-365163, Santa Cruz Biotech); MyoD (NBP1-54153, Novus Biologicals); Ki67 (A21861, ABclonal); MyoG (A21861, ABclonal). Secondary antibodies for fiber and pMPC immunocytochemistry: Donkey Anti-Mouse IgG Secondary Antibody NL 493 conjugated (NL009, Novus Biologicals); Donkey Anti-Rabbit IgG Secondary Antibody NL 493 conjugated (NL006, Novus Biologicals); Donkey Anti-Mouse IgG Secondary Antibody NL 557 conjugated (NL007, Novus Biologicals); Donkey Anti-Rabbit IgG Secondary Antibody NL 637 conjugated (NL005, Novus Biologicals). Primary antibodies for immunohistochemistry of muscle cross sections: Rbl2 (sc-365163, Santa Cruz Biotech). Secondary antibodies for immunohistochemistry of muscle cross sections: Donkey Anti-Mouse IgG Secondary Antibody NL 493 conjugated (NL009, Novus Biologicals)

Statistical Analysis

Statistical analysis was performed using Microsoft Excel. Statistical comparisons between groups were made using two-tailed unpaired Student's t-test. Results are presented as the mean +/- standard deviation (SD) and were considered statistically significant when $p<0.05$.

CHAPTER 4

RESULTS

Rbl2 is required for efficient myogenic differentiation

Genetic deletion or mutation of Rbl2 has been assessed in a whole body mouse model and in humans, respectively (Brunet et al., 2020; Samara et al., 2021; LeCouter et al., 1998; Cobrinik et al., 1996) that showed developmental and musculoskeletal impairment. However, it is not known if dysregulated Rbl2 in MuSCs potentially has a role in the skeletal muscle impairment. To appraise if Rbl2 directly impaired skeletal muscle differentiation, CRISPR/Cas9 was used to generate Rbl2 genetically deleted (Rbl2KO) and control (Ctl) C2C12 myoblast cell lines. The Rbl2KO cell lines were generated by transfecting C2C12 cells using a CRISPR/Cas9 vector with an sgRNA that targets the Rbl2 gene, whereas Ctl cell lines were transfected using a CRISPR/Cas9 vector with a scrambled sgRNA, followed by puromycin selection and expansion **(Fig. 4.1A)**. As Rbl2 protein is not expressed in proliferating cells **(Fig. 4.1B)**, several Rbl2KO and Ctl cell lines were selected by western blotting based on its expression in growth arrested cells **(Fig. 4.1C)**. If Rbl2 is required for myogenic differentiation, impaired myotube formation would be present in the Rbl2KO cell lines compared to Ctl. To test this, Rbl2KO and Ctl cells were differentiated for five days and myotube formation was evaluated using immunofluorescence for the contractile protein myosin heavy chain (MyHC), which is expressed in the late stages of differentiation. Immunofluorescence microscopy revealed more numerous and larger myotube formation in Ctl cells compared to Rbl2KO cells **(Fig. 4.2A)**. The Rbl2KO cells had severely diminished differentiation, with most fields of view absent for any myotube formation. The differentiation potential of Rbl2KO and Ctl cells was measured by assessing the differentiation index, which was

calculated by enumerating the number of nuclei in MyHC+ cells relative to the total number nuclei in a field of view. It was found that Rbl2KO cells had an approximately 19.5-fold reduction in the number of myoblasts that differentiated **(Fig. 4.2B)**. Indeed, only about 2% of Rbl2KO cells expressed MyHC **(Fig. 4.2B)**. The differentiation capacity was measured by assessing the myofusion index, which was calculated by counting the number of nuclei present within myotubes per the number of total myotubes. It was found that Rbl2KO cells had an approximately 8-fold reduction in the average myofusion index compared to Ctl myotubes **(Fig. 4.2C)**. This severely diminished ability of myoblasts to differentiate and the paucity of myotube size suggests that Rbl2 may be crucial for either permitting or instructing the differentiation program. Importantly, it demonstrates an essential requirement of Rbl2 in myogenic differentiation that might account for the whole body mouse and human Rbl2 mutant skeletal muscle phenotypes.

Rbl2 protein is not expressed during quiescence and early activation in MuSCs

As Rbl2 might have a potential function during myoblast differentiation, MuSC fate decisions for activation, self-renewal and commitment to differentiate were also assessed. For this, Rbl2 protein expression was characterized in the course of MuSC fate decisions using mouse extensor digitorum longus (EDL) muscle fibers cultured over various timepoints **(Fig. 4.3A)**. In ex vivo EDL myofiber cultures, all the newly formed cells in clusters originate from only one activated MuSC. At 0 hour, quiescent MuSCs on myofibers co-immunostained for the MuSC quiescent marker Pax7 and Rbl2, revealed that Rbl2 protein was not expressed **(Fig. 4.3B)**. Next, as activation after quiescence of MuSCs is marked by MyoD protein expression, Rbl2 protein expression was investigated during early time points (3, 4, 6 and 8 hours) in culture by co-immunostaining for MyoD and Rbl2. Though MyoD was expressed as early as 3 hours, signifying

that the MuSC activation had occurred, Rbl2 protein was not present **(Fig. 4.3C)**. Together, this data suggests that Rbl2 protein does not have a role during MuSC quiescence, in the initiation of activation and during the early events of activation.

Rbl2 protein is present only in a subset of MyoD+ MuSCs

MuSCs on myofibers were analyzed at 24, 48 and 72 hours post isolation to evaluate Rbl2 protein expression in MuSC clusters where the cells are proliferating, self-renewed or committed. Again, MuSCs were co-immunostained for MyoD and Rbl2. In this case, a subset of MuSCs was found to express Rbl2 protein after 24 hours of culture, which was mostly localized to the nucleus, suggesting that Rbl2 protein is expressed between 8 and 24 hours after activation **(Fig. 4.4)**. Also, the percentage of Rbl2+MyoD+ MuSCs to the total number of MyoD+ MuSCs at 24, 48 and 72 hours were enumerated and found to be 16%, 11% and 15% respectively, suggesting that the Rbl2+ MuSCs are a rare population **(Fig. 4.5)**. Furthermore, the Rbl2+MyoD+ MuSCs occurred almost always in cells that had appeared to have undergone symmetric division, as demonstrated by the planar orientation parallel to the myofiber, suggesting that these are MyoD+Pax7- committed daughter cells **(Fig. 4.4)**. These results support the idea that Rbl2 might have a role in only a subset of MuSCs, corroborating the presence of heterogeneity within the stem cell pool. Alternatively, the orientation of the MyoD+Rbl2+ MuSCs on the fiber might suggest that Rbl2 is expressed only in committed MuSCs.

Thus, Rbl2 protein expression was evaluated to see if it was present in only committed MyoD+ cells by assessing MuSC proliferation status. For this MuSCs were co-immunostained for proliferation marker Ki67 and Rbl2. If Rbl2 is not present in proliferating cells, it would suggest that it is in the fraction of MuSCs that are committed to differentiate. Rbl2 protein was never found

to be expressed with Ki67 in MuSCs of fibers at 24, 48 and 72 hours **(Fig. 4.6)**. As Rbl2+ cells never expressed Ki67, it strongly suggests that Rbl2 protein is only present in the committed MyoD+Pax7- MuSCs. Together, this data indicates that Rbl2 might function during MuSC commitment and differentiation.

Rbl2 protein subcellular localization is altered during MuSC differentiation

To characterize Rbl2 in MuSC differentiation, EDL muscle fibers were cultured for 72 hours before differentiation media was added for 4, 8 and 24 hours to induce differentiation. The differentiating MuSCs were co-immunostained for the differentiation marker MyoG and Rbl2. There was co-immunofluorescence of MyoG and Rbl2 in differentiating MuSCs as early as 4 hours post differentiation **(Fig. 4.7A)**. Interestingly, it was observed that at 24 hours post differentiation, Rbl2 protein localization was outside of the nucleus **(Fig. 4.7A)**. MuSCs quantified for the location of Rbl2 protein, revealed that Rbl2 is only in the nucleus at 4 and 8 hours, whereas the majority (about 73%) is present outside of the nucleus at 24 hours of differentiation **(Fig 4.7B)**. These results show that Rbl2 protein might play a non-canonical role in MuSC differentiation by shifting from the nucleus where it is known to function. Thus, supporting the idea that Rbl2 may function in the mitochondria, as was shown for gene family member Rbl1 in MPCs (Bhattacharya et al., 2021).

Rbl2 protein is localized in the mitochondria of differentiating C2C12 cells

As Rbl2 is required for efficient myogenic differentiation and may be localized in the mitochondria, Rbl2 protein expression was characterized during a C2C12 differentiation time course. Cells were growth arrested and then differentiated over a five day time course to induce myotube formation **(Fig. 4.8A)**. By western blot analysis of whole cell lysates, it was confirmed

that Rbl2 protein is expressed during myogenic differentiation as had been previously demonstrated (Carnac et al., 2000). The Rbl2 protein levels are maintained throughout differentiation, but decrease by day 5 **(Fig. 4.8B)**. These results indicate that Rbl2 protein might be involved in the differentiation process. Next, the subcellular localization of Rbl2 was assessed by western blot analysis of cytoplasmic and mitochondrial lysates of differentiating C2C12 cells. The presence of Rbl2 protein was found in the cytosol of differentiating C2C12 cells and an increase of Rbl2 protein in the mitochondria during differentiation **(Fig. 4.8B)**. These results provide evidence that Rbl2 protein is expressed in the mitochondria during myogenic differentiation where it may have a functional role.

Rbl2 protein is localized in the mitochondria during the differentiation of pMPCs

Rbl2 was then assessed for its presence in the mitochondria of primary MPCs (pMPCs) during differentiation. pMPCs were isolated from MuSCs on EDL myofibers and then cultured on a collagen matrix **(Fig. 4.9A)**. This method allows for the dissociation from any niche specific effects, but provides a model to study differentiation. First, the cells were growth arrested (GA) to determine if the pMPCs behave as the MPC line C2C12. Proliferating and GA cells were immunostained for the proliferation marker Ki67, Rbl2 and with the mitochondria marker, Mitotracker. Surprisingly, confocal microscopy revealed that proliferating (Ki67+) pMPCs, unlike C2C12 cells, expressed Rbl2 protein in the nucleus **(Compare Fig. 4.1B with Fig. 4.9B)**. Furthermore, it was found that GA pMPCs, characterized by the absence of Ki67 expression, expressed Rbl2 protein in the mitochondria **(Fig. 4.9B)**. As GA cells are required for myogenic differentiation, this observation suggests that Rbl2 protein expression in the mitochondria has a role in the differentiation process.

It was then determined if Rbl2 protein has a possible role in the mitochondria during myogenic differentiation. For this, pMPCs were assessed for Rbl2 cellular localization in a time course of differentiation for 2, 4, 6, 12, 24, 48 and 72 hours. The differentiating pMPCs were co-immunostained for mitochondria and for Rbl2 protein expression. Confocal microscopy revealed that Rbl2 protein co-localized with the mitochondria throughout the differentiation time course **(Fig. 4.10)**. This observation is in line with that of differentiating C2C12s (**Fig. 4.8B**) and of differentiating myofiber associated MuSCs (**Fig. 4.7A**). Together this data reveals that Rbl2 may have a mitochondrial role during the differentiation process of pMPCs.

Rbl2 protein is absent from the nucleus during myofiber regeneration

Rbl2 protein expression was then assessed during myogenic differentiation in vivo following muscle regeneration by femoral artery ligation induced injury **(Fig. 4.11A)**. Here, surgery was performed to obstruct blood flow to the lower limbs of a mouse by ligating the femoral artery to the femur of one leg for 4 days. This induces tibialis anterior (TA) muscle damage followed by its regeneration. The TA muscle was isolated and sectioned longitudinally to observe centrally located nuclei, which is indicative of a regenerating fiber and that myogenic differentiation has occurred. The sections were immunostained for Rbl2 and assessed by confocal microscopy. Rbl2 protein was found only outside and between centrally located nuclei of ligated muscle **(Fig. 4.11B)**. This suggests that Rbl2 protein might localize to the mitochondria during myogenic differentiation in vivo, as was shown in vitro. Altogether, the data suggest that Rbl2 has a crucial non-canonical role in the mitochondria during the myogenic differentiation process.

Figure 4.1

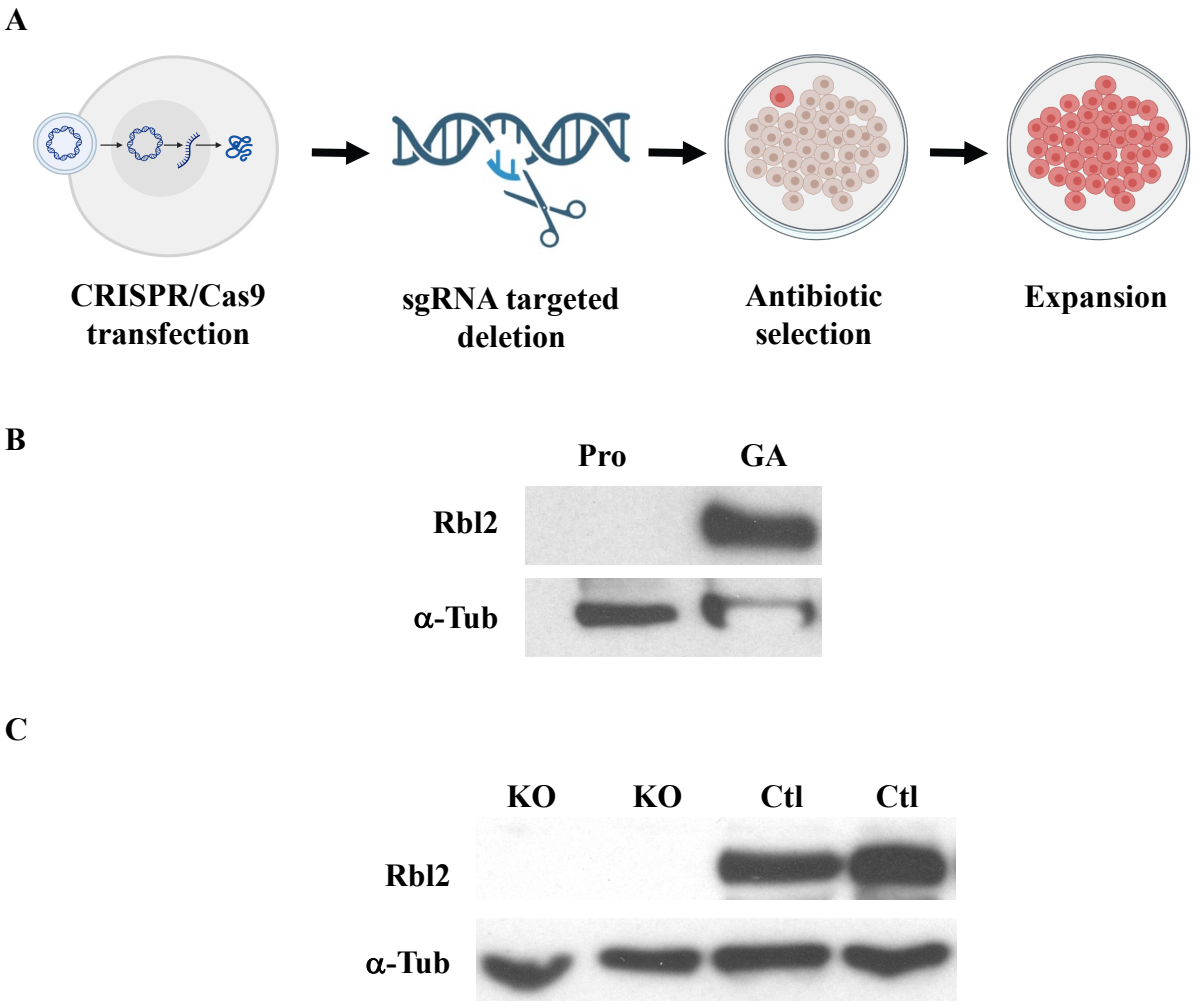

Figure 4.1. Generation of genetically deleted Rbl2 (Rbl2KO) and control (Ctl) cell lines. (A) Schematic demonstrating the method of deriving Rbl2KO and Ctl cell lines. **(B)** Representative western blot of whole cell fractions for Rbl2 and the cytoplasmic loading control α-Tubulin (α-Tub) of proliferating (Pro) and growth arrested (GA) C2C12 cells. **(C)** Representative western blot of Rbl2 and α-Tub for GA Rbl2KO and Ctl C2C12 whole cell lysates, n=3 independent samples.

Figure 4.2

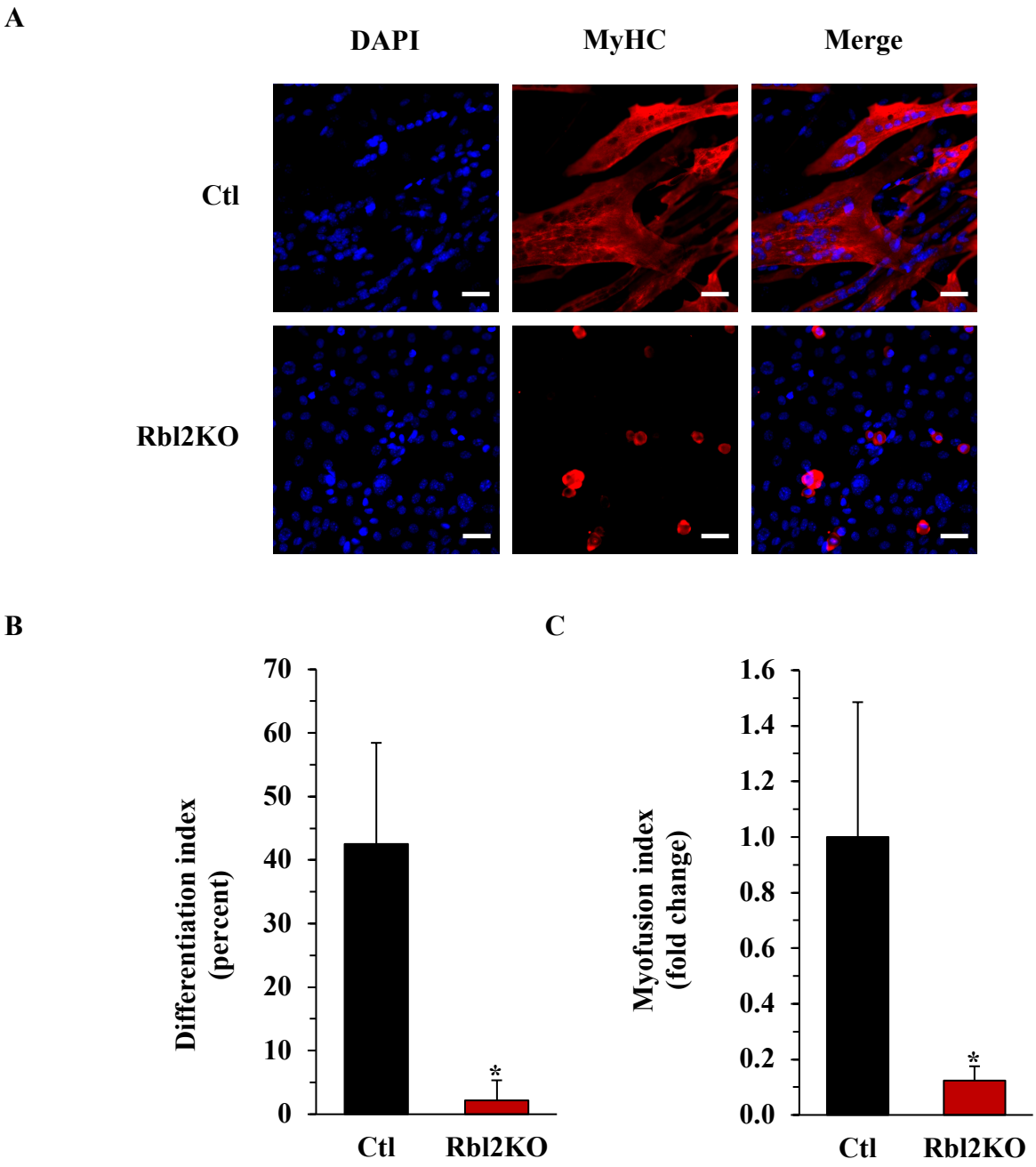

Figure 4.2. Genetic deletion of Rbl2 impairs myogenic differentiation. (A) Representative immunofluorescent microscope images of 5 day differentiated (D5) Ctl and Rbl2KO cells for DAPI, MyHC and Merge (scale bar 40μm). **(B)** Graphical representation of the differentiation index and **(C)** fold change of the myofusion index for D5 Ctl and Rbl2KO cells, n=4-6 independent samples, asterisks denote significance, *p<0.05; Two-tailed unpaired Student's t-test.

Figure 4.3

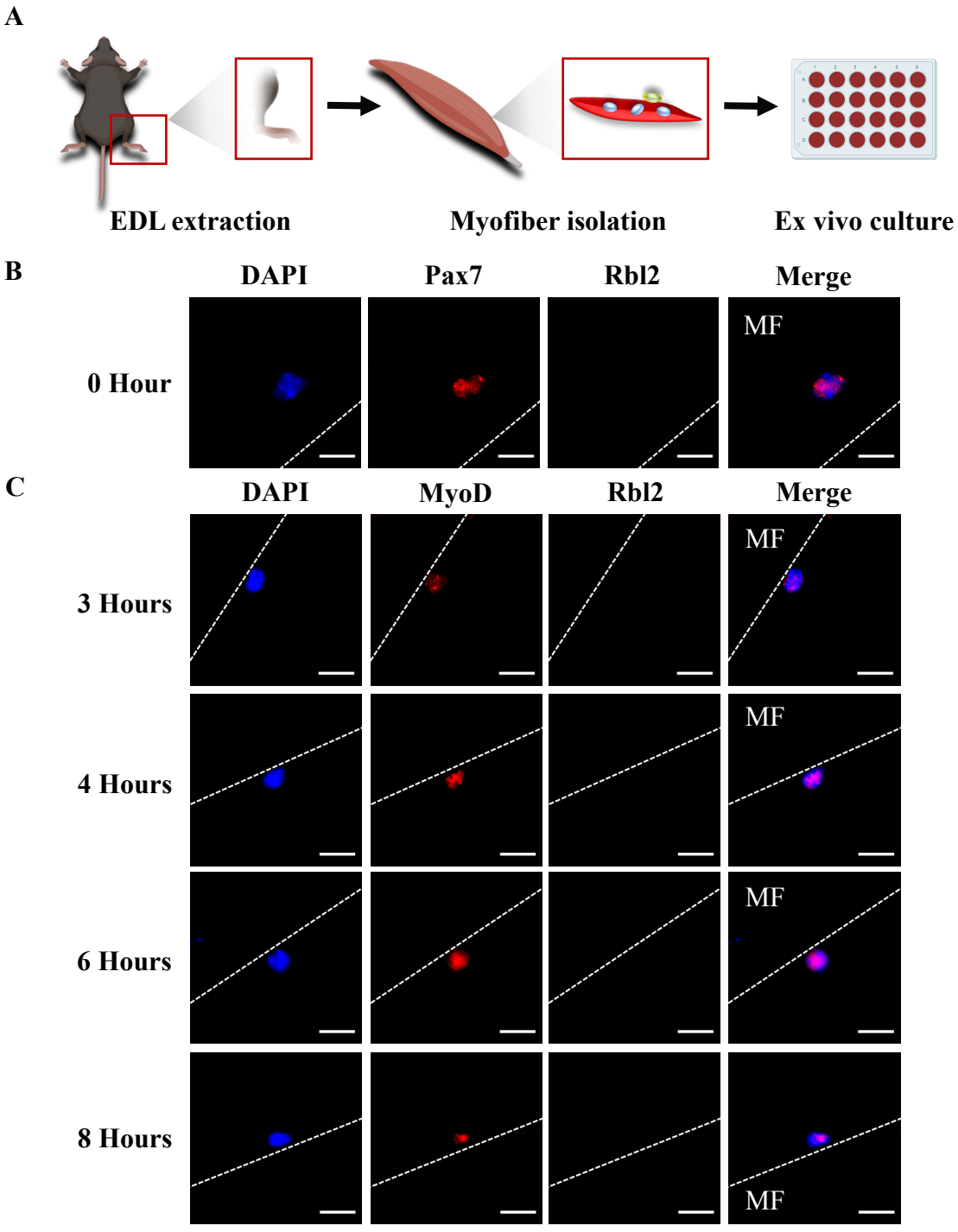

Figure 4.3. Rbl2 protein is not present in quiescent and activated MuSCs up to 8 hours in culture. (A) Schematic demonstrating the methodology of EDL myofiber isolation and culture. Representative immunofluorescent microscope images of EDL myofibers **(B)** at 0 hour in culture for DAPI, Pax7, Rbl2 and Merge and **(C)** at 3, 4, 6, and 8 hours in culture for DAPI, MyoD, Rbl2 and Merge (scale bar 10μm), n=1-2 mice. Myofiber area (MF) is outlined by dashed lines.

Figure 4.4

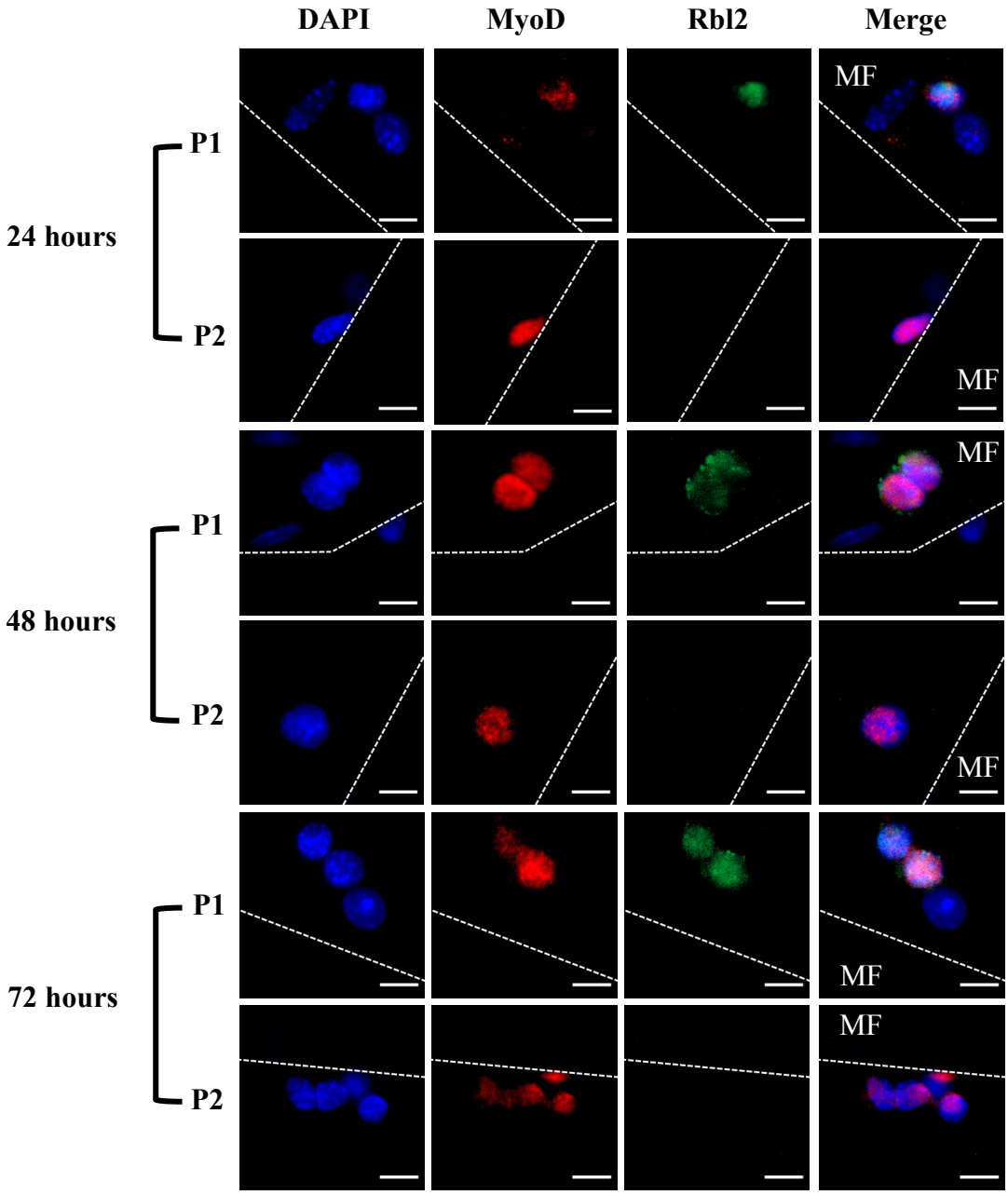

Figure 4.4. Rbl2 protein is present only in a subset of MyoD+ MuSCs. Representative immunofluorescent microscope images of EDL myofibers at 24, 48 and 72 hours in culture for DAPI, MyoD, Rbl2 and Merge (scale bar 10μm), n=1-2 mice. Rbl2+ (P1) and Rbl2- (P2) MuSCs. Myofiber area (MF) is outlined by dashed lines.

Figure 4.5

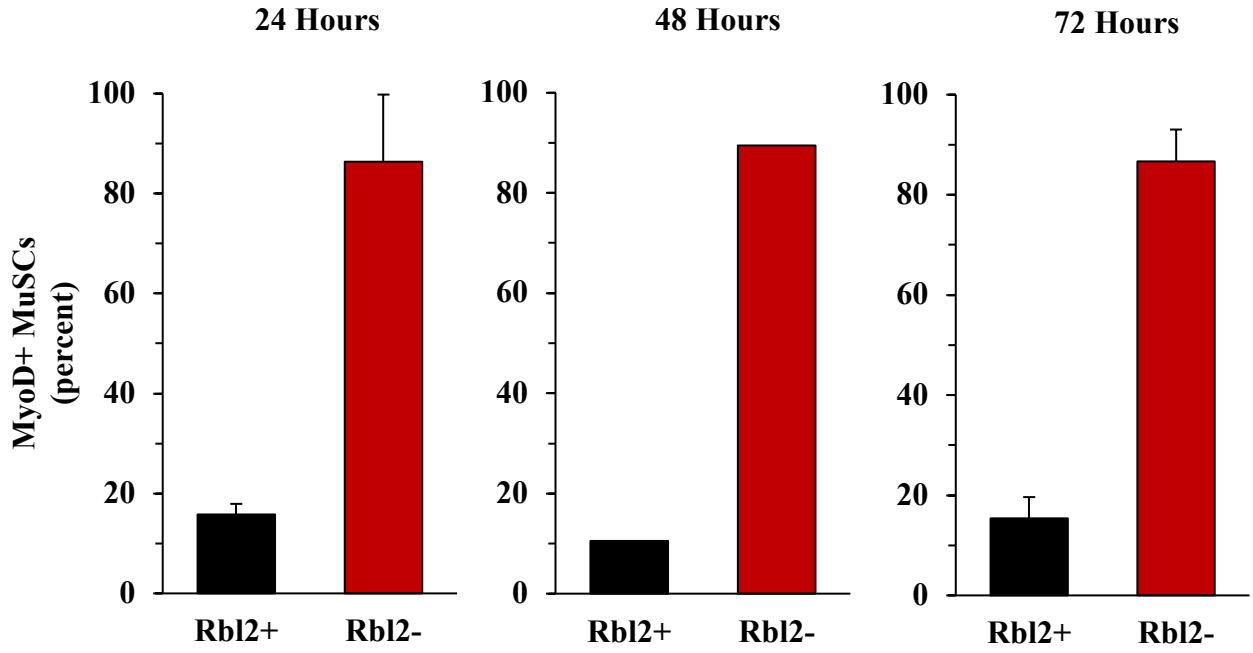

Figure 4.5. Rbl2 protein is present in a rare population of MuSCs that express MyoD. Graphical representation of the relative number of Rbl2 expressing (Rbl2+) and non-expressing (Rbl2-) MyoD+ MuSCs at 24, 48 and 72 hours, n=1-2 mice. Two-tailed unpaired Student's t-test.

Figure 4.6

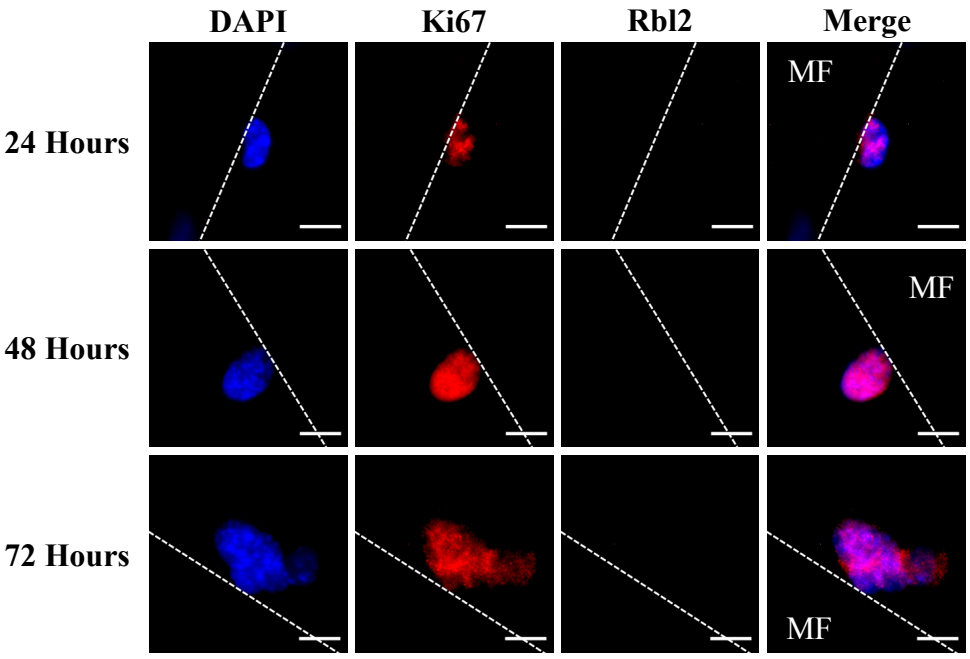

Figure 4.6. Rbl2 protein is not present in proliferating MuSCs. Representative immunofluorescent microscope images of EDL myofibers at 24, 48 and 72 hours in culture for DAPI, Ki67, Rbl2 and Merge (scale bar 10μm), n=1-2 mice. Myofiber area (MF) is outlined by dashed lines.

Figure 4.7

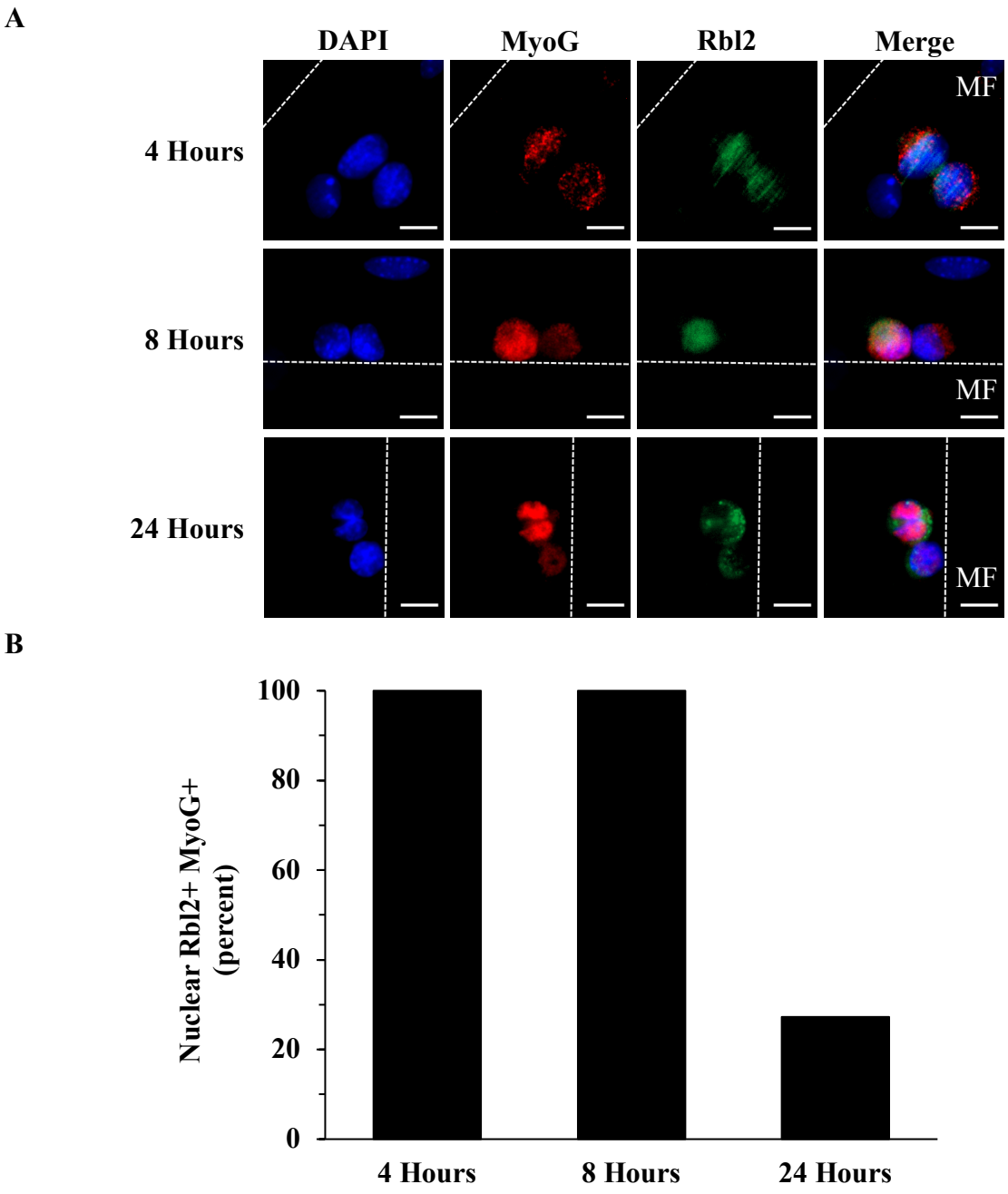

Figure 4.7. Rbl2 protein is present in differentiating MuSCs. (A) Representative immunofluorescent microscope images of EDL myofibers at 4, 8 and 24 hours in differentiation media for DAPI, MyoG, Rbl2 and Merge (scale bar 10μm). Myofiber area (MF) is outlined by dashed lines. **(B)** Graphical representation of the percentage of MyoG+ MuSCs with Rbl2 localized only in the nucleus at 4, 8 and 24 hours in differentiation media, n=1 mouse.

Figure 4.8

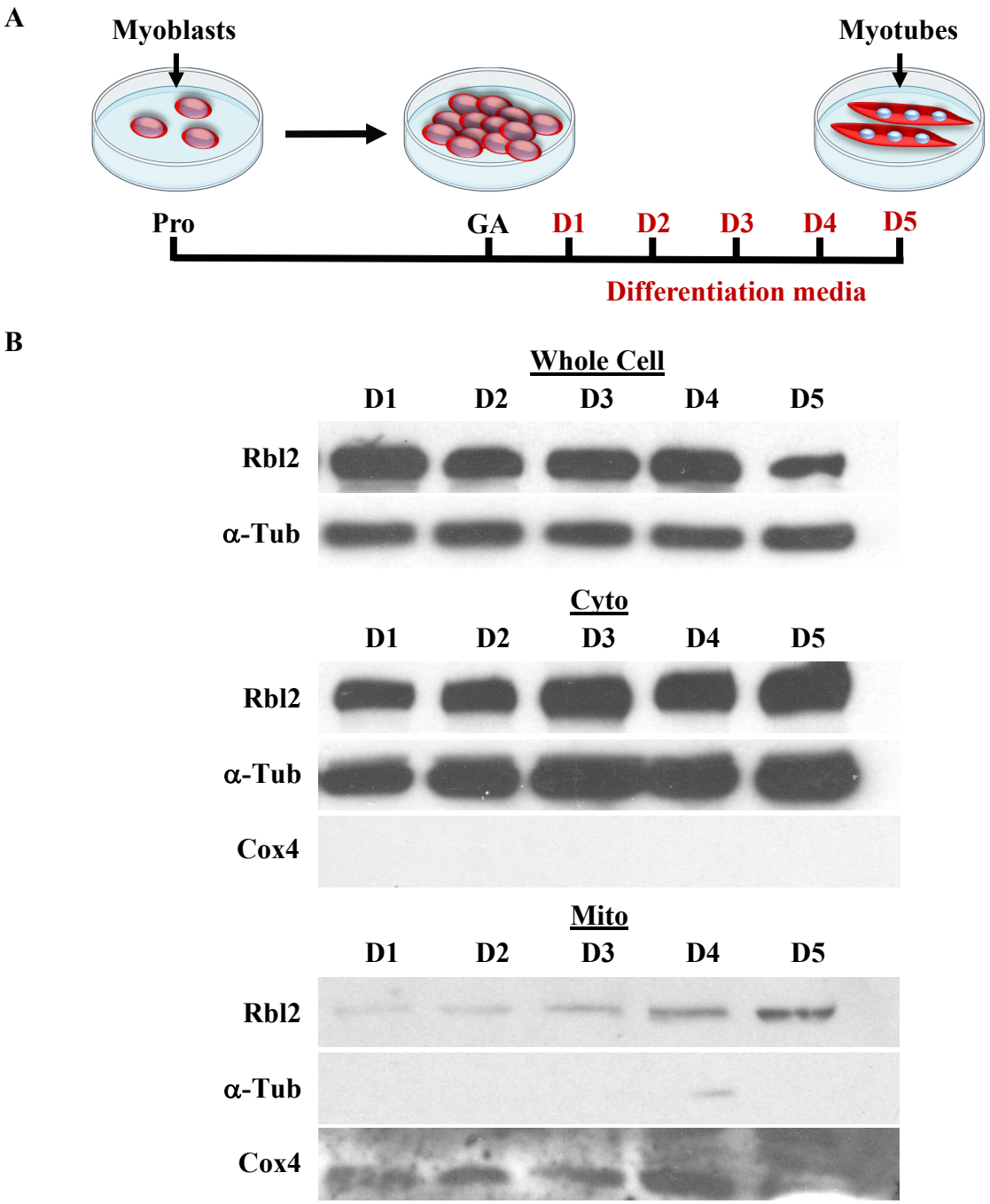

Figure 4.8. Rbl2 protein is present in the mitochondria during the differentiation of C2C12 cells. (A) Schematic demonstrating myoblast proliferation (Pro) and differentiation from 1 to 5 days (D1 through to D5) following growth arrest (GA). **(B)** Representative western blot for Rbl2, α-Tub and Cox4 (mitochondrial loading control) of C2C12 whole cell, cytoplasmic (Cyto) and mitochondrial (Mito) lysates during a five day differentiation time course, n=3 independent samples.

Figure 4.9

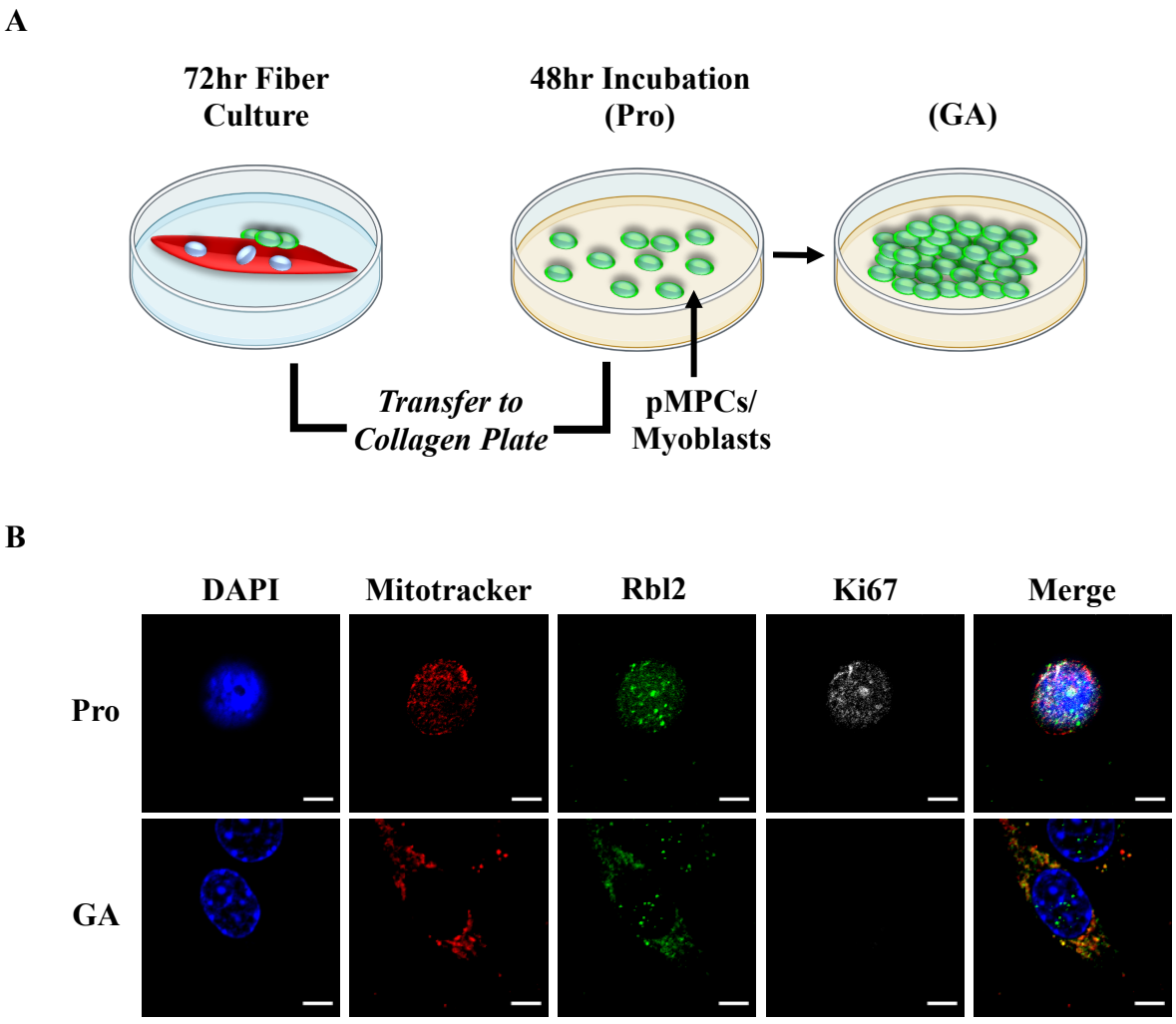

Figure 4.9. Rbl2 protein is localized in the mitochondria during growth arrest of pMPCs. (A) Schematic demonstrating the methodology of primary myogenic progenitor cell (pMPC) isolation from EDL myofibers. **(B)** Representative immunofluorescent confocal microscope images of pMPCs during proliferation (Pro) and growth arrest (GA) for DAPI, Mitotracker, Rbl2, Ki67 and Merge (scale bar 5μm), n=3 mice.

Figure 4.10

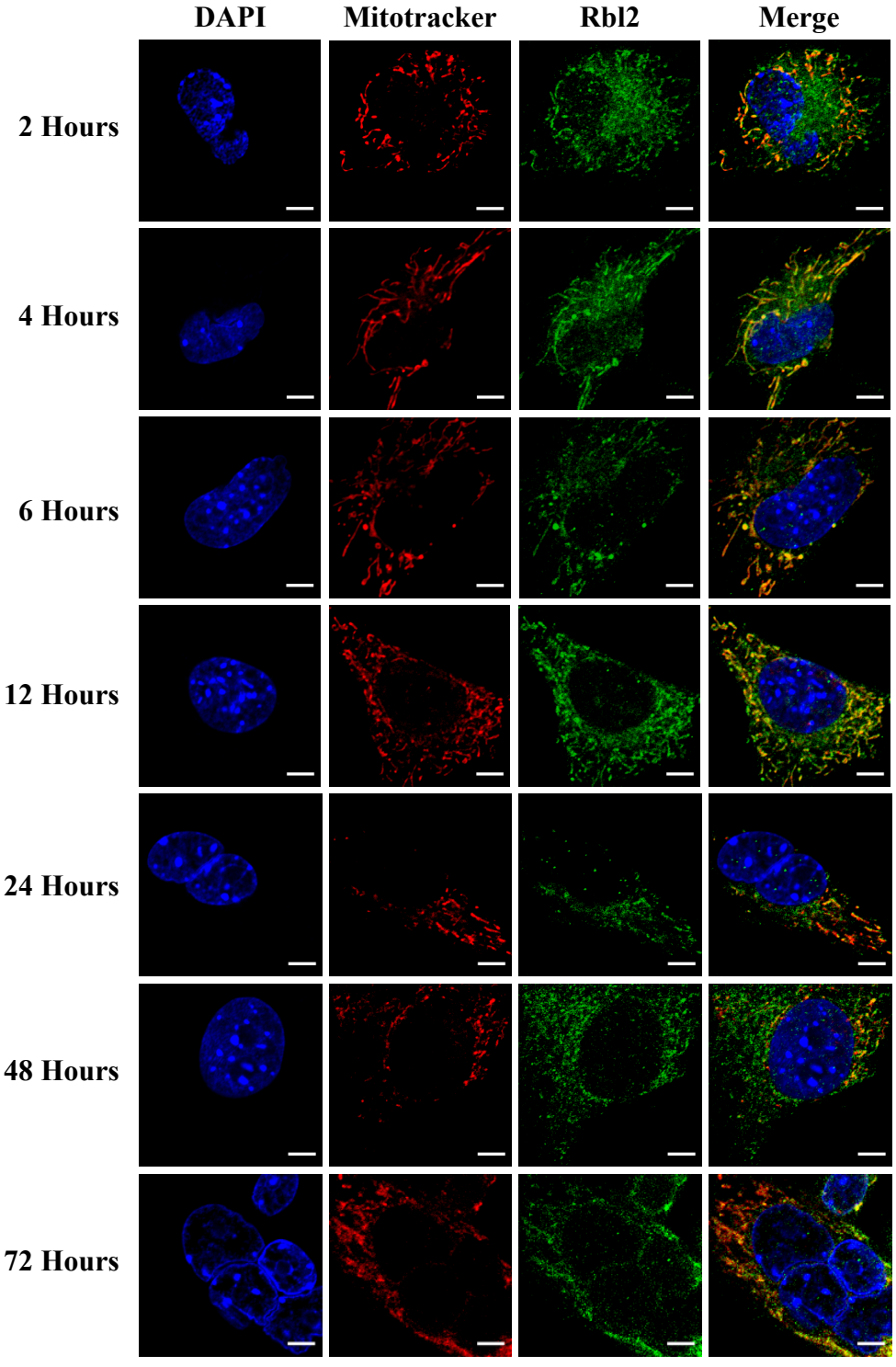

Figure 4.10. Rbl2 protein is present in the in mitochondria of differentiating pMPCs. (A) Representative immunofluorescent confocal microscope images of 2, 4, 6, 12, 24, 48 and 72 hour differentiating pMPCs for DAPI, Mitotracker, Rbl2 and Merge (scale bar 5µm), n=2 mice.

Figure 4.11

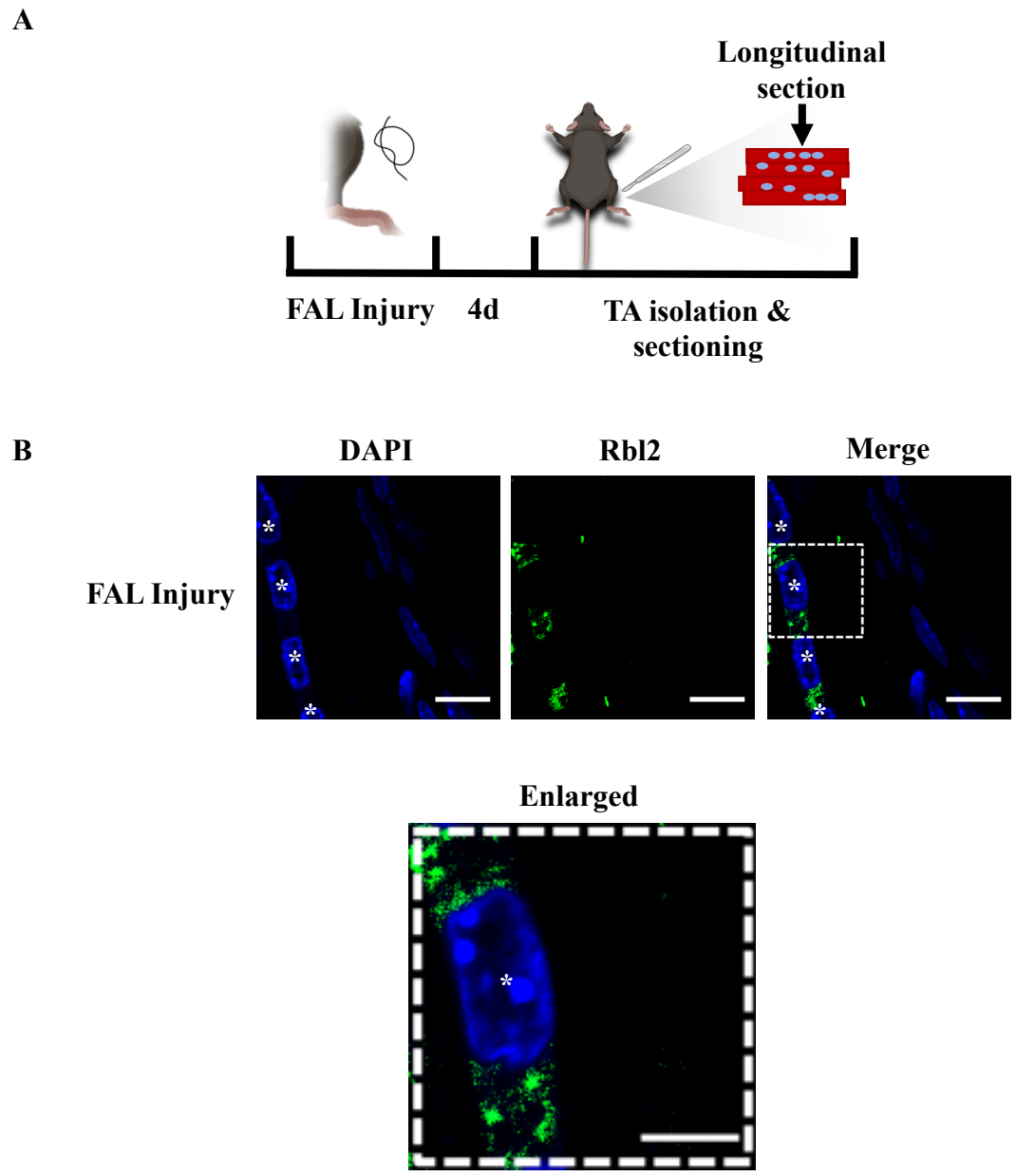

Figure 4.11. Rbl2 protein is present outside of centrally locating nuclei but not peripheral nuclei following 4 day ligation. (A) Schematic demonstrating the methodology of femoral artery ligation (FAL), isolation and sectioning of mouse tibialis anterior (TA) muscle. **(B)** Representative immunofluorescent confocal microscope images of longitudinal sections of FAL injured TA four days after ligation for DAPI, Rbl2 and Merge (scale bar 10μm) and Enlarged merge section (scale bar 5μm), n=2 mice. Asterisks denote centrally located nuclei of a regenerating fiber.

CHAPTER 5

DISCUSSION

Despite the evidence implicating the retinoblastoma susceptibility gene family member, Rbl2, in skeletal muscular disorder and developmental abnormalities (LeCouter et al., 1998; Brunet et al., 2020; Samara et al., 2021), a thorough investigation and characterization of Rbl2 in MuSC fate decisions has only been done in this study. Rbl2 might have multiple roles for MuSC fate decisions and during the differentiation process **(Fig. 5.1).** For the first time, these results implicate Rbl2 as an important protein involved in MuSC fate decisions and has a novel mitochondrial role during myogenic differentiation. Notably, it was found that Rbl2 genetic deletion (Rbl2KO) in C2C12 myoblasts resulted in impaired myotube formation **(Fig. 4.2A)**, with deficits in differentiation potential (lower differentiation index) (**Fig. 4.2B)** and differentiation capacity (lower myofusion index) **(Fig. 4.2C)** compared to control. Thus, this latest understanding of Rbl2 may eventually provide a potential avenue for treating and understanding aging and muscle wasting diseases where MuSC malfunction in fate decisions and muscle breakdown is prevalent.

This thesis is the first to evaluate Rbl2 protein in MuSCs of myofibers. The onset of Rbl2 protein expression occurred in the nucleus of only a rare subset of MuSCs beginning after 8 hours in culture **(Fig. 4.4)**. The percentage of Rbl2+ MuSCs is in line with the levels of the MuSC population that had never expressed Myf5- (Kuang et al., 2007) **(Fig. 4.5)**. Moreover, by assessing Ki67 expression at later timepoints when MuSCs form clusters with progenies of different myogenic fates (Pasut et al., 2013; Hüttner et al., 2021), proliferating MuSCs did not express Rbl2, but a subset of MyoD+ cells did **(Fig. 4.4 & 4.6)**. Thus, the MuSCs that were Rbl2-, but were expressing MyoD, might be proliferating MuSCs, and the MyoD+Rbl2+ MuSCs were committed to differentiate. Interestingly, when MuSCs were removed from their niche by plating pMPCs

separate from their myofibers, Rbl2 protein was expressed in the nucleus of a subset of cells **(Fig. 4.9B)**. This suggests the possibility that the cells without its niche provided by the myofibers became committed and mimic the committed population of MuSCs on myofibers. Committed cells (MyoD+Pax7-) are known to continue to proliferate but are all destined to differentiate (Zammit et al., 2006). A shortcoming of this study was that Pax7 expression was not evaluated for the MuSCs on the fiber. If the conclusion that committed and differentiating MuSCs are the only populations that express Rbl2 is correct, then MuSCs should be Rbl2+MyoD+Pax7-.

To properly study the role of Rbl2 in MuSCs it would be prudent to use a conditional genetic deletion of Rbl2 specifically in MuSCs. In this case, Rbl2 Cre-loxP mice can be mated to the Pax7Cre-eRT mice such that the addition of Tamoxifen would only express cre recombinase in MuSCs so that Rbl2 could be genetically mutated. This method would ensure that any observations are MuSC specific and as Rbl2 whole body genetic deletions in the Black/6 strain are lethal, it would ensure that the mouse develops and provides viable MuSCs (LeCouter et al., 1998). In vivo, it is expected that there would be a smaller cross-sectional area and fewer differentiating MuSCs in Rbl2 mutants compared to wild type mice.

When evaluating Rbl2 protein expression during the course of MuSC fate decisions on isolated myofibers, Rbl2 protein is mostly expressed in the nucleus of a minority subpopulation of committed MuSCs **(Fig. 4.4 & 4.5)**. However, during the differentiation process, Rbl2 is located outside of the nucleus of MuSCs **(Fig. 4.7A & 4.7B).** Moreover, its presence was demonstrated in the mitochondria of differentiating C2C12 myoblasts **(Fig. 4.8B)** and primary myogenic progenitor cells (pMPCs) **(Fig. 4.10)**. Furthermore, during skeletal muscle regeneration, Rbl2 protein is expressed outside and between centrally located nuclei of regenerating muscle **(Fig. 4.11B)**. Rbl2 is hypothesized to be involved in MuSC differentiation through a mitochondrial function, given

that it is expressed in the mitochondria only at that time, and because its deletion is impairs muscle formation **(Fig. 5.1)**.

Importantly, this study can explain the severe skeletal muscle defects described in humans with Rbl2 mutation. The notable phenotype included impaired growth and development, and muscle hypotonia in humans, which was also apparent in mice (LeCouter et al., 1998; Brunet et al., 2020; Samara et al., 2021). Moreover, in mice (dependent on the strain background) there was a reduced number of differentiated myocytes (LeCouter et al., 1998; Cobrinik et al., 1996). As presented in this thesis, targeted deletion of Rbl2 in C2C12 cells had significantly less differentiated myotubes that were strikingly smaller (**Fig. 4.2A, 4.2B & 4.2C)**. Thus, the central impairments caused by Rbl2 loss is hypothesized to be the differentiation capacity of MuSCs. To further verify that Rbl2 is required for differentiation, future experiments will aim to rescue the defects observed in Rbl2KO cells. This can be achieved by transfecting Rbl2KO cells with plasmids containing Rbl2 to determine if differentiation returns to control levels. If the differentiation deficits are restored, this will further substantiate the evidence that Rbl2 has a function in differentiation.

It is well understood that Rbl2 is present during quiescence of many cell types where it functions in the nucleus to repress cell cycle dependent genes (Litovchick et al., 2007; Popov et al., 2020). Rbl2 protein expression was not found in any myonuclei. For its presence in quiescent MuSCs, there is limited and conflicting evidence from other studies that Rbl2 is expressed. In one report, Fukada et al did not find Rbl2 gene expression in quiescent pMPCs, but in another study Rbl2 was upregulated in a population of RCs (Fukada et al., 2007; Carnac et al., 2000). In agreement with the former study, Rbl2 protein was not detected ex vivo in quiescent MuSCs **(Fig. 4.3B)**. This suggests that Rbl2 protein does not have a role in maintaining MuSC quiescence. The

differentiation of pMPCs did not yield any RCs, as all the cells had differentiated, so that the findings could not be substantiated in quiescent RCs. If Rbl2 is upregulated in RCs it might suggest that RCs are primed to commit once stimulated, as it was found that Rbl2 is expressed in committed MuSCs **(Fig. 4.4)**. Also, these results indicate that RCs do not substantially mimic quiescent MuSCs that is most likely a result of lacking a myofiber niche, which undoubtedly regulates several MuSC processes (Kann et al., 2021). Future studies should assess the differences between quiescent MuSCs and RCs.

Rbl2 protein is not expressed during the proliferation of C2C12 cells or in proliferating MuSCs **(Fig. 4.1B & 4.6)**. Contrary to this, a study found that Rbl2 was present in proliferating C2C12 myoblasts, but at almost undetectable levels (Carnac et al., 2000). The miniscule presence of Rbl2 may be caused by a population of growth arrested C2C12 cells expressing Rbl2 as was demonstrated **(Fig 4.1B)**. Indeed, it is unclear whether Rbl2 was present in a phosphorylated state, as its increased phosphorylation would have a bearing on the validity of its presence during proliferation (Carnac et al., 2000). Alternatively, as presented in this thesis, Rbl2 protein could have been expressed during proliferation but at very low amounts, which went undetected. It was also found that Rbl2 transcript is present in proliferating C2C12 cells (Carnac et al., 2000). Rbl2 transcript may be present, but its translation repressed. It is well established that both Myf5 and MyoD transcript can be present in quiescent MuSCs, but their translation is prevented until activation to allow for rapid myogenic commitment when needed (Crist et al., 2012; Morée et al., 2017).

Interestingly, there has been evidence showing that overexpression of Rbl2 in proliferating C2C12 myoblasts prevents cell cycle progression and inhibits differentiation by preventing MyoD expression, which is contradictory to the results of this thesis showing that Rbl2 is required for

differentiation (Carnac et al., 2000). Rbl2 may operate within a tightly regulated window where there exists an optimal concentration and timepoint for it to function, which might explain the results in the C2C12 cells. Thus, manipulating the concentration and/or timing of Rbl2 inappropriately would cause the inhibition of differentiation. Whereas this thesis describes a possible functional role of Rbl2 in the mitochondria for differentiation, the study by Carnac et al did not provide any data regarding the localization of the transfected Rbl2 protein (Carnac et al., 2000). Rbl2 may not have localized to the mitochondria where it might have influenced the onset of differentiation. To reconcile these differences, it would be a worthwhile investigation to find if MuSCs behave the same way as the C2C12 cells, by transfecting MuSCs on EDL myofibers in culture with Rbl2 and mitochondria targeted Rbl2 to assess proliferation and fate decisions.

As Rbl2 has not been investigated in the mitochondria of MuSCs and Rbl1 mitochondrial function is implicated in fate decisions, it is hypothesized that Rbl2 functions in MuSCs by interacting in the mitochondria. For the first time, this study provides evidence for a non-canonical role of Rbl2 in MuSCs, functioning in the mitochondria as opposed to its canonical role where it is known to function in the nucleus. Indeed, during differentiation of MuSCs, Rbl2 was present outside of the nucleus in MuSCs and during muscle regeneration **(Fig. 4.7A & 4.11B)** and localization in the mitochondria of MPCs and pMPCs **(Fig. 4.8B & 4.10)**.

It has been proposed that mitochondria should be understood as information processing systems. First, they sense and respond to endogenous and environmental inputs by remodeling, then integrate this information through dynamic, network-based physical interactions and diffusion mechanisms, finally producing an output signal that affect the functions of other organelles and regulate physiology (Picard & Shirihai, 2022). Rbl2 appears to regulate MuSC fate decisions through the mitochondria. The fact that Rbl2 might play a non-canonical role in MuSC

differentiation by its absence from the nucleus where it is known to function, is not an unreasonable supposition. The Rb family members Rb1 and Rbl1 have been shown to interact at the mitochondria during proliferation (Ferecatu et al., 2009; Hilgendorf et al., 2013; Bhattacharya et al., 2021). Rb1 has been shown to localize to the outer mitochondrial membrane where it activates bcl-2-like protein 4 (BAX) and induces BAX-mediated membrane permeabilization and cytochrome *c* release to induce apoptosis (Hilgendorf et al., 2013). For Rbl1, it was demonstrated to influence proliferative fates of MPCs through a mitochondrial function (Bhattacharya et al., 2021). Here, Rbl1 directly binds to the mitochondrial DNA (mtDNA) where it reduces mitochondrial gene transcription for electron transport chain (ETC) proteins and reduces OXPHOS generation that decreases the MPC proliferation rate (Bhattacharya et al., 2021). A basic local alignment search tool analysis of mouse Rb1 and Rbl2 show a 24.26% sequence similarity, with a greater homology between mouse Rbl1 and Rbl2 (48.51% sequence similarity). This suggests that Rbl2 may act more similarly to Rbl1 than Rb1. To evaluate whether Rbl2 works to affect fate decisions in a similar manner as Rbl1, chromatin immunoprecipitation of Rbl2 on mtDNA of MPCs can be used to determine if Rbl2 is interacting at the mtDNA to repress transcription of ETC complex genes, just as Rbl1 does.

How Rbl2 potentially influences the mitochondria to affect fate decisions has yet to be determined. Though, there has been mounting evidence implicating mitochondria in stem cell fate decisions (Khacho et al., 2016; Hong et al*.,* 2022; Bhattacharya et al*.,* 2021). Studies have shown that mitochondrial remodelling takes place during myogenic differentiation. Mitochondria upregulate fission related proteins in the early stages of differentiation to allow for mitochondrial clearance and reformation of mitochondrial networks to provide differentiated muscle the OXPHOS needed to sustain energy intensive tasks (Sin et al., 2016; Kim et al., 2013). Importantly

for differentiation, altering mitochondrial fragmentation and fission related proteins can delay or permit myogenic differentiation (De Palma et al., 2010; Sin et al., 2016). Rbl1 has been shown to alter mitochondrial dynamics and OXPHOS to influence MPC proliferation (Bhattacharya et al., 2021). Genetic deletion of Rbl1 (Rbl1KO) in MPCs, resulted in increased mitochondrial networking and proliferation (Bhattacharya et al., 2021). Thus, it is possible that Rbl2 is mediating myogenic differentiation by altering mitochondrial dynamics during differentiation. To test this hypothesis, the mitochondrial network of Rbl2KO cells should be assessed during a differentiation time course. It would be expected that Rbl2KO cells would not readily undergo mitochondrial fragmentation during differentiation. Furthermore, increased ROS levels have been associated with myogenic differentiation (Malinska et al., 2012; L'honoré et al., 2018) and may be the mechanism in which mitochondria signal for differentiation (Yu et al., 2006; Jheng et al., 2012). The ROS levels between Rbl2KO and control cells can be compared and determined by treating with a mitochondrial ROS indicator such as dihydrorhodamine 123 and observing for fluorescence using flow cytometry analysis. If Rbl2 influences differentiation through ROS, then control cells should have a greater signal than Rbl2KO cells.

Proteins destined for the mitochondria require specialized transport through N-terminal targeting signals that direct them to their respective mitochondrial subcompartment (Hansen & Herrmann, 2019). It is unclear how Rbl2 is transported into to the mitochondrial matrix as it lacks an N-terminal targeting sequence. Some proteins destined for the mitochondria have been shown to have internal mitochondrial translocation signal-like structures that improve import efficiency such as Rbl1 (Backes et al., 2018; Bhattacharya et al., 2021).

In summary, these findings relate Rbl2 to MuSC fate, as well as a potential mitochondrial function during differentiation **(Fig. 5.1)**. It was determined that Rbl2 protein is absent during

quiescence, early activation and proliferation of MuSCs, but is present during commitment and the differentiation process. Here, Rbl2 protein location changes from being primarily observed in the nucleus of committed MuSCs, to the mitochondria during differentiation. The absence of Rbl2 significantly impairs myogenic differentiation, which suggests that Rbl2 has a crucial function. Rbl2 was also observed in vivo during muscle regeneration which presents an opportunity for targeted regenerative medicine applications in skeletal muscle disorders.

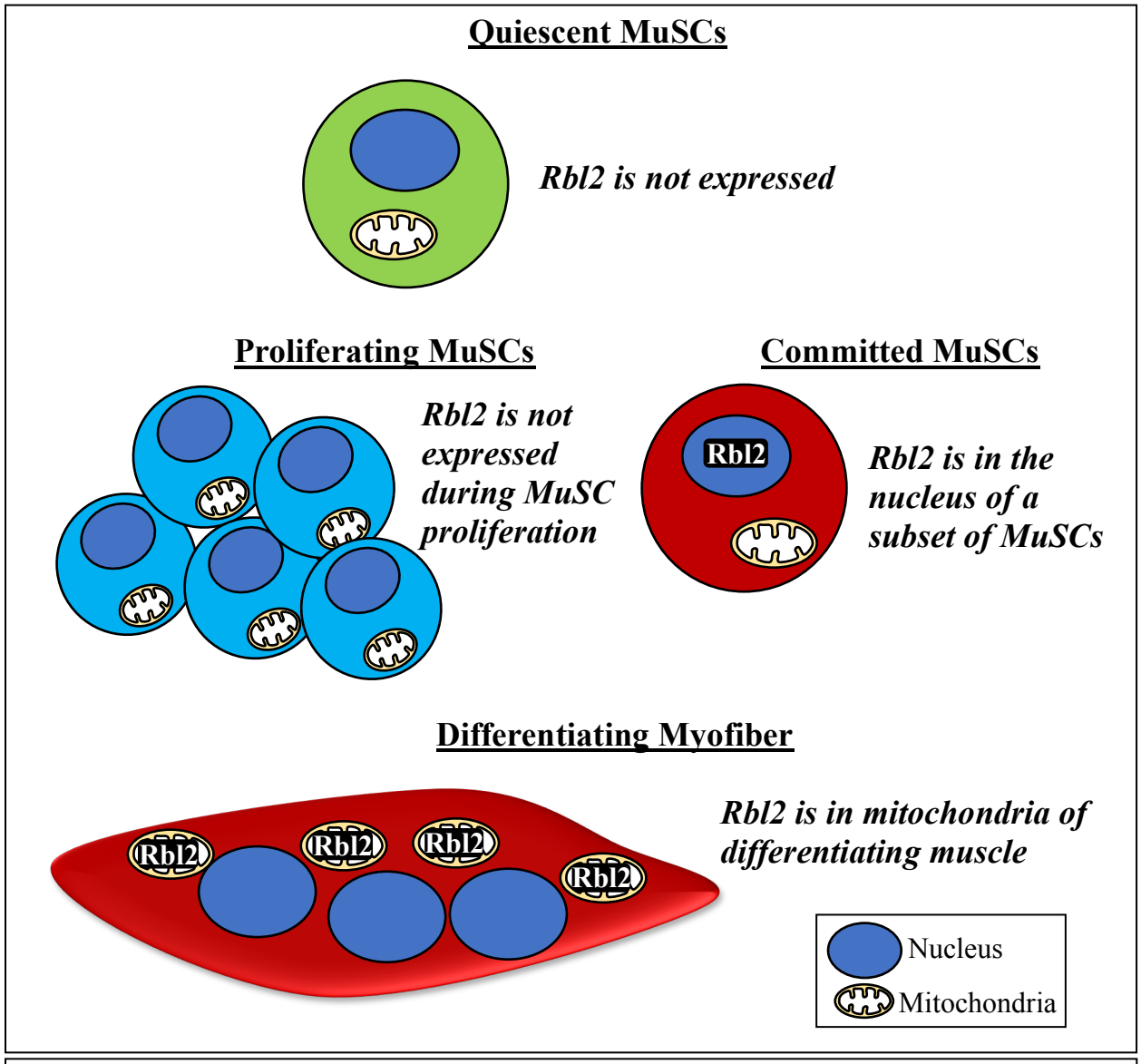

Figure 5.1. Characterization of Rbl2 in MuSC fate decisions. Rbl2 protein is not expressed during quiescence or proliferation, but presents itself in the nucleus of committing MuSCs. During myogenic differentiation, Rbl2 protein is present in the mitochondria.

CHAPTER 6

REFERENCES

Abate, M., Festa, A., Falco, M., Lombardi, A., Luce, A., Grimaldi, A., Zappavigna, S., Sperlongano, P., Irace, C., Caraglia, M., & Misso, G. (2020). Mitochondria as playmakers of apoptosis, autophagy and senescence. *Seminars in cell & developmental biology*, *98*, 139–153.

Abou-Khalil, R., Le Grand, F., & Chazaud, B. (2013). Human and murine skeletal muscle reserve cells. *Methods in molecular biology (Clifton, N.J.)*, *1035*, 165–177.

Ancel, S., Stuelsatz, P., & Feige, J. N. (2021). Muscle stem cell quiescence: Controlling stemness by staying asleep. *Trends in cell biology*, *31*(7), 556–568.

Backes, S., Hess, S., Boos, F., Woellhaf, M. W., Gödel, S., Jung, M., Mühlhaus, T., & Herrmann, J. M. (2018). Tom70 enhances mitochondrial preprotein import efficiency by binding to internal targeting sequences. *The Journal of cell biology*, *217*(4), 1369–1382.

Ban-Ishihara, R., Ishihara, T., Sasaki, N., Mihara, K., & Ishihara, N. (2013). Dynamics of nucleoid structure regulated by mitochondrial fission contributes to cristae reformation and release of cytochrome c. *Proceedings of the National Academy of Sciences of the United States of America*, *110*(29), 11863–11868.

Benezra, R., Davis, R. L., Lockshon, D., Turner, D. L., & Weintraub, H. (1990). The protein Id: a negative regulator of helix-loop-helix DNA binding proteins. *Cell*, *61*(1), 49–59.

Berry, B. J., Trewin, A. J., Amitrano, A. M., Kim, M., & Wojtovich, A. P. (2018). Use the protonmotive force: Mitochondrial uncoupling and reactive oxygen species. *Journal of molecular biology*, *430*(21), 3873–3891.

Bhattacharya, D., & Scimè, A. (2020). Mitochondrial function in muscle stem cell fates. *Frontiers in cell and developmental biology*, *8*, 480.

Bhattacharya, D., Shah, V., Oresajo, O., & Scimè, A. (2021). p107 mediated mitochondrial function controls muscle stem cell proliferative fates. *Nature communications*, *12*(1), 5977.

Bianconi, V., & Mozzetta, C. (2022). Epigenetic control of muscle stem cells: time for a new dimension. *Trends in genetics*, *38*(5), 501–513.

Bischoff R. (1986). Proliferation of muscle satellite cells on intact myofibers in culture. *Developmental biology*, *115*(1), 129–139.

Brieger, K., Schiavone, S., Miller, F. J., Jr, & Krause, K. H. (2012). Reactive oxygen species: from health to disease. *Swiss medical weekly*, *142*, w13659.

Brun, C. E., Wang, Y. X., & Rudnicki, M. A. (2018). Single EDL myofiber isolation for analyses of quiescent and activated muscle stem cells. *Methods in molecular biology*, *1686*, 149–159.

Brunet, T., Radivojkov-Blagojevic, M., Lichtner, P., Kraus, V., Meitinger, T., & Wagner, M. (2020). Biallelic loss-of-function variants in RBL2 in siblings with a neurodevelopmental disorder. *Annals of clinical and translational neurology*, *7*(3), 390–396.

Cadonic, C., Sabbir, M. G., & Albensi, B. C. (2016). Mechanisms of mitochondrial dysfunction in Alzheimer's disease. *Molecular neurobiology*, *53*(9), 6078–6090.

Cadot, B., Gache, V., Vasyutina, E., Falcone, S., Birchmeier, C., & Gomes, E. R. (2012). Nuclear movement during myotube formation is microtubule and dynein dependent and is regulated by Cdc42, Par6 and Par3. *EMBO reports*, *13*(8), 741–749.

Cao, Y., Kumar, R. M., Penn, B. H., Berkes, C. A., Kooperberg, C., Boyer, L. A., Young, R. A., & Tapscott, S. J. (2006). Global and gene-specific analyses show distinct roles for Myod and Myog at a common set of promoters. *The EMBO journal*, *25*(3), 502–511.

Carnac, G., Fajas, L., L'honoré, A., Sardet, C., Lamb, N. J., & Fernandez, A. (2000). The retinoblastoma-like protein p130 is involved in the determination of reserve cells in differentiating myoblasts. *Current biology*, *10*(9), 543–546.

Chakkalakal, J. V., Christensen, J., Xiang, W., Tierney, M. T., Boscolo, F. S., Sacco, A., & Brack, A. S. (2014). Early forming label-retaining muscle stem cells require p27kip1 for maintenance of the primitive state. *Development*, *141*(8), 1649–1659.

Chakkalakal, J. V., Jones, K. M., Basson, M. A., & Brack, A. S. (2012). The aged niche disrupts muscle stem cell quiescence. *Nature*, *490*(7420), 355–360.

Chandel, N. S., McClintock, D. S., Feliciano, C. E., Wood, T. M., Melendez, J. A., Rodriguez, A. M., & Schumacker, P. T. (2000). Reactive oxygen species generated at mitochondrial complex III stabilize hypoxia-inducible factor-1alpha during hypoxia: a mechanism of O2 sensing. *The Journal of biological chemistry*, *275*(33), 25130–25138.

Chapman, M. A., Zhang, J., Banerjee, I., Guo, L. T., Zhang, Z., Shelton, G. D., Ouyang, K., Lieber, R. L., & Chen, J. (2014). Disruption of both nesprin 1 and desmin results in nuclear anchorage defects and fibrosis in skeletal muscle. *Human molecular genetics*, *23*(22), 5879–5892.

Classon, M., & Dyson, N. (2001). p107 and p130: versatile proteins with interesting pockets. *Experimental cell research*, *264*(1), 135–147.

Cobrinik D. (2005). Pocket proteins and cell cycle control. *Oncogene*, *24*(17), 2796–2809.

Cobrinik, D., Lee, M. H., Hannon, G., Mulligan, G., Bronson, R. T., Dyson, N., Harlow, E., Beach, D., Weinberg, R. A., & Jacks, T. (1996). Shared role of the pRB-related p130 and p107 proteins in limb development. *Genes & development*, *10*(13), 1633–1644.

Conboy, I. M., Conboy, M. J., Wagers, A. J., Girma, E. R., Weissman, I. L., & Rando, T. A. (2005). Rejuvenation of aged progenitor cells by exposure to a young systemic environment. *Nature*, *433*(7027), 760–764.

Cosgrove, B. D., Gilbert, P. M., Porpiglia, E., Mourkioti, F., Lee, S. P., Corbel, S. Y., Llewellyn, M. E., Delp, S. L., & Blau, H. M. (2014). Rejuvenation of the muscle stem cell population restores strength to injured aged muscles. *Nature medicine*, *20*(3), 255–264.

Crist, C. G., Montarras, D., & Buckingham, M. (2012). Muscle satellite cells are primed for myogenesis but maintain quiescence with sequestration of Myf5 mRNA targeted by microRNA-31 in mRNP granules. *Cell stem cell*, *11*(1), 118–126.

Cruz-Jentoft, A. J., & Sayer, A. A. (2019). Sarcopenia. *Lancet*, *393*(10191), 2636–2646.

Davie, J. K., Cho, J. H., Meadows, E., Flynn, J. M., Knapp, J. R., & Klein, W. H. (2007). Target gene selectivity of the myogenic basic helix-loop-helix transcription factor myogenin in embryonic muscle. *Developmental biology*, *311*(2), 650–664.

De Palma, C., Falcone, S., Pisoni, S., Cipolat, S., Panzeri, C., Pambianco, S., Pisconti, A., Allevi, R., Bassi, M. T., Cossu, G., Pozzan, T., Moncada, S., Scorrano, L., Brunelli, S., & Clementi, E. (2010). Nitric oxide inhibition of Drp1-mediated mitochondrial fission is critical for myogenic differentiation. *Cell death and differentiation*, *17*(11), 1684–1696.

De Sousa, M., Porras, D. P., Perry, C. G., Seale, P., & Scimè, A. (2014). p107 is a crucial regulator for determining the adipocyte lineage fate choices of stem cells. *Stem cells*, *32*(5), 1323–1336.

Dumont, N. A., Bentzinger, C. F., Sincennes, M. C., & Rudnicki, M. A. (2015a). Satellite cells and skeletal muscle regeneration. *Comprehensive physiology*, *5*(3), 1027–1059.

Dumont, N. A., Wang, Y. X., & Rudnicki, M. A. (2015c). Intrinsic and extrinsic mechanisms regulating satellite cell function. *Development*, *142*(9), 1572–1581.

Dumont, N. A., Wang, Y. X., Von Maltzahn, J., Pasut, A., Bentzinger, C. F., Brun, C. E., & Rudnicki, M. A. (2015b). Dystrophin expression in muscle stem cells regulates their polarity and asymmetric division. *Nature medicine*, *21*(12), 1455–1463.

Emery A. E. (2002). The muscular dystrophies. *Lancet*, *359*(9307), 687–695.

Espigat-Georger, A., Dyachuk, V., Chemin, C., Emorine, L., & Merdes, A. (2016). Nuclear alignment in myotubes requires centrosome proteins recruited by nesprin-1. *Journal of cell science*, *129*(22), 4227–4237.

Feige, P., Brun, C. E., Ritso, M., & Rudnicki, M. A. (2018). Orienting muscle stem cells for regeneration in homeostasis, aging, and disease. *Cell stem cell*, *23*(5), 653–664.

Fenton, A. R., Jongens, T. A., & Holzbaur, E. L. F. (2021). Mitochondrial dynamics: Shaping and remodeling an organelle network. *Current opinion in cell biology*, *68*, 28–36.

Ferecatu, I., Le Floch, N., Bergeaud, M., Rodríguez-Enfedaque, A., Rincheval, V., Oliver, L., Vallette, F. M., Mignotte, B., & Vayssière, J. L. (2009). Evidence for a mitochondrial localization of the retinoblastoma protein. *BMC cell biology*, *10*, 50.

Filippelli, R. L., & Chang, N. C. (2022). Empowering muscle stem cells for the treatment of Duchenne muscular dystrophy. *Cells, tissues, organs*, *211*(6), 641–654.

Fischer, M., & Müller, G. A. (2017). Cell cycle transcription control: DREAM/MuvB and RB-E2F complexes. *Critical reviews in biochemistry and molecular biology*, *52*(6), 638–662.

Flores, M., & Goodrich, D. W. (2022). Retinoblastoma protein paralogs and tumor suppression. *Frontiers in genetics*, *13*, 818719.

Folmes, C. D., Dzeja, P. P., Nelson, T. J., & Terzic, A. (2012). Metabolic plasticity in stem cell homeostasis and differentiation. *Cell stem cell*, *11*(5), 596–606.

Frolov, M. V., & Dyson, N. J. (2004). Molecular mechanisms of E2F-dependent activation and pRB-mediated repression. *Journal of cell science*, *117*(Pt 11), 2173–2181.

Frontera, W. R., & Ochala, J. (2015). Skeletal muscle: a brief review of structure and function. *Calcified tissue international*, *96*(3), 183–195.

Fukada, S., Uezumi, A., Ikemoto, M., Masuda, S., Segawa, M., Tanimura, N., Yamamoto, H., Miyagoe-Suzuki, Y., & Takeda, S. (2007). Molecular signature of quiescent satellite cells in adult skeletal muscle. *Stem cells*, *25*(10), 2448–2459.

García-Prat, L., Perdiguero, E., Alonso-Martín, S., Dell'Orso, S., Ravichandran, S., Brooks, S. R., Juan, A. H., Campanario, S., Jiang, K., Hong, X., Ortet, L., Ruiz-Bonilla, V., Flández, M., Moiseeva, V., Rebollo, E., Jardí, M., Sun, H. W., Musarò, A., Sandri, M., Del Sol, A., Sartorelli, V., Muñoz-Cánoves, P. (2020). FoxO maintains a genuine muscle stem-cell quiescent state until geriatric age. *Nature cell biology*, *22*(11), 1307–1318.

Gayraud-Morel, B., Chrétien, F., Jory, A., Sambasivan, R., Negroni, E., Flamant, P., Soubigou, G., Coppée, J. Y., Di Santo, J., Cumano, A., Mouly, V., & Tajbakhsh, S. (2012). Myf5 haploinsufficiency reveals distinct cell fate potentials for adult skeletal muscle stem cells. *Journal of cell science*, *125*(Pt 7), 1738–1749.

Glancy, B., Hartnell, L. M., Malide, D., Yu, Z. X., Combs, C. A., Connelly, P. S., Subramaniam, S., & Balaban, R. S. (2015). Mitochondrial reticulum for cellular energy distribution in muscle. *Nature*, *523*(7562), 617–620.

Halevy, O., Novitch, B. G., Spicer, D. B., Skapek, S. X., Rhee, J., Hannon, G. J., Beach, D., & Lassar, A. B. (1995). Correlation of terminal cell cycle arrest of skeletal muscle with induction of p21 by MyoD. *Science*, *267*(5200), 1018–1021.

Hansen, K. G., & Herrmann, J. M. (2019). Transport of proteins into mitochondria. *The protein journal*, *38*(3), 330–342.

Hasty, P., Bradley, A., Morris, J. H., Edmondson, D. G., Venuti, J. M., Olson, E. N., & Klein, W. H. (1993). Muscle deficiency and neonatal death in mice with a targeted mutation in the myogenin gene. *Nature*, *364*(6437), 501–506.

Henley, S. A., & Dick, F. A. (2012). The retinoblastoma family of proteins and their regulatory functions in the mammalian cell division cycle. *Cell division*, *7*(1), 10.

Hernández-Hernández, J. M., García-González, E. G., Brun, C. E., & Rudnicki, M. A. (2017). The myogenic regulatory factors, determinants of muscle development, cell identity and regeneration. *Seminars in cell & developmental biology*, *72*, 10–18.

Hilgendorf, K. I., Leshchiner, E. S., Nedelcu, S., Maynard, M. A., Calo, E., Ianari, A., Walensky, L. D., & Lees, J. A. (2013). The retinoblastoma protein induces apoptosis directly at the mitochondria. *Genes & development*, *27*(9), 1003–1015.

Hoffmann, C., Höckele, S., Kappler, L., Hrabě de Angelis, M., Häring, H. U., & Weigert, C. (2018). The effect of differentiation and TGFβ on mitochondrial respiration and mitochondrial enzyme abundance in cultured primary human skeletal muscle cells. *Scientific reports*, *8*(1), 737.

Hollenberg, S. M., Cheng, P. F., & Weintraub, H. (1993). Use of a conditional MyoD transcription factor in studies of MyoD trans-activation and muscle determination. *Proceedings of the national academy of sciences of the United States of America*, *90*(17), 8028–8032.

Hong, X., Isern, J., Campanario, S., Perdiguero, E., Ramírez-Pardo, I., Segalés, J., Hernansanz-Agustín, P., Curtabbi, A., Deryagin, O., Pollán, A., González-Reyes, J. A., Villalba, J. M., Sandri, M., Serrano, A. L., Enríquez, J. A., & Muñoz-Cánoves, P. (2022). Mitochondrial dynamics maintain muscle stem cell regenerative competence throughout adult life by regulating metabolism and mitophagy. *Cell stem cell*, *29*(9), 1298–1314.e10.

Hori, S., Hiramuki, Y., Nishimura, D., Sato, F., & Sehara-Fujisawa, A. (2019). PDH-mediated metabolic flow is critical for skeletal muscle stem cell differentiation and myotube formation during regeneration in mice. *FASEB journal*, *33*(7), 8094–8109.

Hüttner, S. S., Hayn, C., Ahrens, H. E., Schmidt, M., Henze, H., & von Maltzahn, J. (2021). Single myofiber culture assay for the assessment of adult muscle stem cell functionality ex vivo. *JoVE*, (168), 10.3791/62257.

Hwang, A. B., & Brack, A. S. (2018). Muscle stem cells and aging. *Current topics in developmental biology*, *126*, 299–322.

Jheng, H. F., Tsai, P. J., Guo, S. M., Kuo, L. H., Chang, C. S., Su, I. J., Chang, C. R., & Tsai, Y. S. (2012). Mitochondrial fission contributes to mitochondrial dysfunction and insulin resistance in skeletal muscle. *Molecular and cellular biology*, *32*(2), 309–319.

Kann, A. P., Hung, M., & Krauss, R. S. (2021). Cell-cell contact and signaling in the muscle stem cell niche. *Current opinion in cell biology*, *73*, 78–83.

Khacho, M., Clark, A., Svoboda, D. S., Azzi, J., MacLaurin, J. G., Meghaizel, C., Sesaki, H., Lagace, D. C., Germain, M., Harper, M. E., Park, D. S., & Slack, R. S. (2016). Mitochondrial dynamics impacts stem cell identity and fate decisions by regulating a nuclear transcriptional program. *Cell stem cell*, *19*(2), 232–247.

Kim, B., Kim, J. S., Yoon, Y., Santiago, M. C., Brown, M. D., & Park, J. Y. (2013). Inhibition of Drp1-dependent mitochondrial division impairs myogenic differentiation. *American journal of physiology. Regulatory, integrative and comparative physiology*, *305*(8), R927–R938.

Knottnerus, S. J. G., Bleeker, J. C., Wüst, R. C. I., Ferdinandusse, S., IJlst, L., Wijburg, F. A., Wanders, R. J. A., Visser, G., & Houtkooper, R. H. (2018). Disorders of mitochondrial long-chain fatty acid oxidation and the carnitine shuttle. *Reviews in endocrine & metabolic disorders*, *19*(1), 93–106.

Kuang, S., Chargé, S. B., Seale, P., Huh, M., & Rudnicki, M. A. (2006). Distinct roles for Pax7 and Pax3 in adult regenerative myogenesis. *The Journal of cell biology*, *172*(1), 103–113.

Kuang, S., Kuroda, K., Le Grand, F., & Rudnicki, M. A. (2007). Asymmetric self-renewal and commitment of satellite stem cells in muscle. *Cell*, *129*(5), 999–1010.

Latil, M., Rocheteau, P., Châtre, L., Sanulli, S., Mémet, S., Ricchetti, M., Tajbakhsh, S., & Chrétien, F. (2012). Skeletal muscle stem cells adopt a dormant cell state post mortem and retain regenerative capacity. *Nature communications*, *3*, 903.

Le Grand, F., Jones, A. E., Seale, V., Scimè, A., & Rudnicki, M. A. (2009). Wnt7a activates the planar cell polarity pathway to drive the symmetric expansion of satellite stem cells. *Cell stem cell*, *4*(6), 535–547.

LeCouter, J. E., Kablar, B., Whyte, P. F., Ying, C., & Rudnicki, M. A. (1998). Strain-dependent embryonic lethality in mice lacking the retinoblastoma-related p130 gene. *Development (Cambridge, England)*, *125*(23), 4669–4679.

Lehka, L., & Rędowicz, M. J. (2020). Mechanisms regulating myoblast fusion: A multilevel interplay. *Seminars in cell & developmental biology*, *104*, 81–92.

Lei, K., Zhang, X., Ding, X., Guo, X., Chen, M., Zhu, B., Xu, T., Zhuang, Y., Xu, R., & Han, M. (2009). SUN1 and SUN2 play critical but partially redundant roles in anchoring nuclei in skeletal muscle cells in mice. *Proceedings of the national academy of sciences of the United States of America*, *106*(25), 10207–10212.

L'honoré, A., Commère, P. H., Negroni, E., Pallafacchina, G., Friguet, B., Drouin, J., Buckingham, M., & Montarras, D. (2018). The role of Pitx2 and Pitx3 in muscle stem cells gives new insights into P38α MAP kinase and redox regulation of muscle regeneration. *eLife*, *7*, e32991.

L'honoré, A., Commère, P. H., Ouimette, J. F., Montarras, D., Drouin, J., & Buckingham, M. (2014). Redox regulation by Pitx2 and Pitx3 is critical for fetal myogenesis. *Developmental cell*, *29*(4), 392–405.

Li, L., Chen, Y., & Gibson, S. B. (2013). Starvation-induced autophagy is regulated by mitochondrial reactive oxygen species leading to AMPK activation. *Cellular signalling*, *25*(1), 50–65.

Liban, T. J., Medina, E. M., Tripathi, S., Sengupta, S., Henry, R. W., Buchler, N. E., & Rubin, S. M. (2017). Conservation and divergence of C-terminal domain structure in the retinoblastoma protein family. *Proceedings of the national academy of sciences of the United States of America*, *114*(19), 4942–4947.

Liban, T. J., Thwaites, M. J., Dick, F. A., & Rubin, S. M. (2016). Structural conservation and E2F binding specificity within the retinoblastoma pocket protein family. *Journal of molecular biology*, *428*(20), 3960–3971.

Lim, C. B., Prêle, C. M., Baltic, S., Arthur, P. G., Creaney, J., Watkins, D. N., Thompson, P. J., & Mutsaers, S. E. (2015). Mitochondria-derived reactive oxygen species drive GANT61-induced mesothelioma cell apoptosis. *Oncotarget*, *6*(3), 1519–1530.

Litovchick, L., Sadasivam, S., Florens, L., Zhu, X., Swanson, S. K., Velmurugan, S., Chen, R., Washburn, M. P., Liu, X. S., & DeCaprio, J. A. (2007). Evolutionarily conserved multisubunit RBL2/p130 and E2F4 protein complex represses human cell cycle-dependent genes in quiescence. *Molecular cell*, *26*(4), 539–551.

Łukasik, P., Załuski, M., & Gutowska, I. (2021). Cyclin-Dependent Kinases (CDK) and Their Role in Diseases Development-Review. *International journal of molecular sciences*, *22*(6), 2935.

Lunt, S. Y., & Vander Heiden, M. G. (2011). Aerobic glycolysis: meeting the metabolic requirements of cell proliferation. *Annual review of cell and developmental biology*, *27*, 441–464.

Malinska, D., Kudin, A. P., Bejtka, M., & Kunz, W. S. (2012). Changes in mitochondrial reactive oxygen species synthesis during differentiation of skeletal muscle cells. *Mitochondrion*, *12*(1), 144–148.

Mansouri, A., Stoykova, A., Torres, M., & Gruss, P. (1996). Dysgenesis of cephalic neural crest derivatives in Pax7-/- mutant mice. *Development*, *122*(3), 831–838.

Martínez-Reyes, I., & Chandel, N. S. (2020). Mitochondrial TCA cycle metabolites control physiology and disease. *Nature communications*, *11*(1), 102.

Mauro, A. (1961). Satellite cell of skeletal muscle fibers. *The Journal of biophysical and biochemical cytology*, *9*(2), 493–495.

Megeney, L. A., Kablar, B., Garrett, K., Anderson, J. E., & Rudnicki, M. A. (1996). MyoD is required for myogenic stem cell function in adult skeletal muscle. *Genes & development*, *10*(10), 1173–1183.

Mercuri, E., Bönnemann, C. G., & Muntoni, F. (2019). Muscular dystrophies. *Lancet, 394*(10213), 2025–2038.

Metzger, T., Gache, V., Xu, M., Cadot, B., Folker, E. S., Richardson, B. E., Gomes, E. R., & Baylies, M. K. (2012). MAP and kinesin-dependent nuclear positioning is required for skeletal muscle function. *Nature*, *484*(7392), 120–124.

Mitchell P. (1961). Coupling of phosphorylation to electron and hydrogen transfer by a chemi-osmotic type of mechanism. *Nature*, *191*, 144–148.

Morrée, A., van Velthoven, C. T. J., Gan, Q., Salvi, J. S., Klein, J. D. D., Akimenko, I., Quarta, M., Biressi, S., & Rando, T. A. (2017). Staufen1 inhibits MyoD translation to actively maintain muscle stem cell quiescence. *Proceedings of the national academy of sciences of the United States of America*, *114*(43), E8996–E9005.

Nabeshima, Y., Hanaoka, K., Hayasaka, M., Esumi, E., Li, S., Nonaka, I., & Nabeshima, Y. (1993). Myogenin gene disruption results in perinatal lethality because of severe muscle defect. *Nature*, *364*(6437), 532–535.

Nicholls, T. J., & Gustafsson, C. M. (2018). Separating and segregating the human mitochondrial Genome. *Trends in biochemical sciences*, *43*(11), 869–881.

Ono, Y., Masuda, S., Nam, H. S., Benezra, R., Miyagoe-Suzuki, Y., & Takeda, S. (2012). Slow-dividing satellite cells retain long-term self-renewal ability in adult muscle. *Journal of cell science*, *125*(Pt 5), 1309–1317.

Oyewole, A. O., & Birch-Machin, M. A. (2015). Mitochondria-targeted antioxidants. *FASEB journal*, *29*(12), 4766–4771.

Pala, F., Di Girolamo, D., Mella, S., Yennek, S., Chatre, L., Ricchetti, M., & Tajbakhsh, S. (2018). Distinct metabolic states govern skeletal muscle stem cell fates during prenatal and postnatal myogenesis. *Journal of cell science*, *131*(14), jcs212977.

Pasut, A., Jones, A. E., & Rudnicki, M. A. (2013). Isolation and culture of individual myofibers and their satellite cells from adult skeletal muscle. *JoVE*, (73), e50074.

Pfanner, N., Warscheid, B., & Wiedemann, N. (2019). Mitochondrial proteins: from biogenesis to functional networks. *Nature reviews. Molecular cell biology*, *20*(5), 267–284.

Picard, M., & Shirihai, O. S. (2022). Mitochondrial signal transduction. *Cell metabolism*, *34*(11), 1620–1653.

Popov, B., Petrov, N., Ryabov, V., & Evsyukov, I. (2020). p130 and pRb in the maintenance of transient quiescence of mesenchymal stem cells. *Stem cells international*, *2020*, 8883436.

Porras, D. P., Abbaszadeh, M., Bhattacharya, D., D'Souza, N. C., Edjiu, N. R., Perry, C. G. R., & Scimè, A. (2017). p107 determines a metabolic checkpoint required for adipocyte lineage fates. *Stem cells*, *35*(5), 1378–1391.

Price, F. D., von Maltzahn, J., Bentzinger, C. F., Dumont, N. A., Yin, H., Chang, N. C., Wilson, D. H., Frenette, J., & Rudnicki, M. A. (2014). Inhibition of JAK-STAT signaling stimulates adult satellite cell function. *Nature medicine*, *20*(10), 1174–1181.

Qiu, H., Liu, N., Luo, L., Zhong, J., Tang, Z., Kang, K., Qu, J., Peng, W., Liu, L., Li, L., & Gou, D. (2016). MicroRNA-17-92 regulates myoblast proliferation and differentiation by targeting the ENH1/Id1 signaling axis. *Cell death and differentiation*, *23*(10), 1658–1669.

Rahman, F. A., & Quadrilatero, J. (2021). Mitochondrial network remodeling: an important feature of myogenesis and skeletal muscle regeneration. *CMLS*, *78*(10), 4653–4675.

Relaix, F., Rocancourt, D., Mansouri, A., & Buckingham, M. (2005). A Pax3/Pax7-dependent population of skeletal muscle progenitor cells. *Nature*, *435*(7044), 948–953.

Remels, A. H., Langen, R. C., Schrauwen, P., Schaart, G., Schols, A. M., & Gosker, H. R. (2010). Regulation of mitochondrial biogenesis during myogenesis. *Molecular and cellular endocrinology*, *315*(1-2), 113–120.

Rochard, P., Rodier, A., Casas, F., Cassar-Malek, I., Marchal-Victorion, S., Daury, L., Wrutniak, C., & Cabello, G. (2000). Mitochondrial activity is involved in the regulation of myoblast differentiation through myogenin expression and activity of myogenic factors. *The Journal of biological chemistry*, *275*(4), 2733–2744.

Rocheteau, P., Gayraud-Morel, B., Siegl-Cachedenier, I., Blasco, M. A., & Tajbakhsh, S. (2012). A subpopulation of adult skeletal muscle stem cells retains all template DNA strands after cell division. *Cell*, *148*(1-2), 112–125.

Rodgers, J. T., King, K. Y., Brett, J. O., Cromie, M. J., Charville, G. W., Maguire, K. K., Brunson, C., Mastey, N., Liu, L., Tsai, C. R., Goodell, M. A., & Rando, T. A. (2014). mTORC1 controls the adaptive transition of quiescent stem cells from G0 to G(Alert). *Nature*, *510*(7505), 393–396.

Roman, W., & Gomes, E. R. (2018). Nuclear positioning in skeletal muscle. *Seminars in cell & developmental biology*, *82*, 51–56.

Roman, W., Martins, J. P., Carvalho, F. A., Voituriez, R., Abella, J. V. G., Santos, N. C., Cadot, B., Way, M., & Gomes, E. R. (2017). Myofibril contraction and crosslinking drive nuclear movement to the periphery of skeletal muscle. *Nature cell biology*, *19*(10), 1189–1201.

Ryall, J. G., Dell'Orso, S., Derfoul, A., Juan, A., Zare, H., Feng, X., Clermont, D., Koulnis, M., Gutierrez-Cruz, G., Fulco, M., & Sartorelli, V. (2015). The NAD(+)-dependent SIRT1 deacetylase translates a metabolic switch into regulatory epigenetics in skeletal muscle stem cells. *Cell stem cell*, *16*(2), 171–183.

Samra, N., Toubiana, S., Yttervik, H., Tzur-Gilat, A., Morani, I., Itzkovich, C., Giladi, L., Abu Jabal, K., Cao, J. Z., Godley, L. A., Mory, A., Baris Feldman, H., Tveten, K., Selig, S., & Weiss, K. (2021). RBL2 bi-allelic truncating variants cause severe motor and cognitive impairment without evidence for abnormalities in DNA methylation or telomeric function. *Journal of human genetics*, *66*(11), 1101–1112.

Schmidt, M., Schüler, S. C., Hüttner, S. S., von Eyss, B., & von Maltzahn, J. (2019). Adult stem cells at work: regenerating skeletal muscle. *CMLS*, *76*(13), 2559–2570.

Scimè, A., Grenier, G., Huh, M. S., Gillespie, M. A., Bevilacqua, L., Harper, M. E., & Rudnicki, M. A. (2005). Rb and p107 regulate preadipocyte differentiation into white versus brown fat through repression of PGC-1alpha. *Cell metabolism*, *2*(5), 283–295.

Seale, P., Sabourin, L. A., Girgis-Gabardo, A., Mansouri, A., Gruss, P., & Rudnicki, M. A. (2000). Pax7 is required for the specification of myogenic satellite cells. *Cell*, *102*(6), 777–786.

Seyer, P., Grandemange, S., Busson, M., Carazo, A., Gamaléri, F., Pessemesse, L., Casas, F., Cabello, G., & Wrutniak-Cabello, C. (2006). Mitochondrial activity regulates myoblast differentiation by control of c-Myc expression. *Journal of cellular physiology*, *207*(1), 75–86.

Seyer, P., Grandemange, S., Rochard, P., Busson, M., Pessemesse, L., Casas, F., Cabello, G., & Wrutniak-Cabello, C. (2011). P43-dependent mitochondrial activity regulates myoblast differentiation and slow myosin isoform expression by control of Calcineurin expression. *Experimental cell research*, *317*(14), 2059–2071.

Shintaku, J., Peterson, J. M., Talbert, E. E., Gu, J. M., Ladner, K. J., Williams, D. R., Mousavi, K., Wang, R., Sartorelli, V., & Guttridge, D. C. (2016). MyoD regulates skeletal muscle oxidative metabolism cooperatively with alternative NF-κB. *Cell reports*, *17*(2), 514–526.

Sin, J., Andres, A. M., Taylor, D. J., Weston, T., Hiraumi, Y., Stotland, A., Kim, B. J., Huang, C., Doran, K. S., & Gottlieb, R. A. (2016). Mitophagy is required for mitochondrial biogenesis and myogenic differentiation of C2C12 myoblasts. *Autophagy*, *12*(2), 369–380.

Smith, C. K., 2nd, Janney, M. J., & Allen, R. E. (1994). Temporal expression of myogenic regulatory genes during activation, proliferation, and differentiation of rat skeletal muscle satellite cells. *Journal of cellular physiology*, *159*(2), 379–385.

Sugihara, H., Teramoto, N., Nakamura, K., Shiga, T., Shirakawa, T., Matsuo, M., Ogasawara, M., Nishino, I., Matsuwaki, T., Nishihara, M., & Yamanouchi, K. (2020). Cellular senescence-mediated exacerbation of Duchenne muscular dystrophy. *Scientific reports*, *10*(1), 16385.

Sun, L., Trausch-Azar, J. S., Ciechanover, A., & Schwartz, A. L. (2005). Ubiquitin-proteasome-mediated degradation, intracellular localization, and protein synthesis of MyoD and Id1 during muscle differentiation. *The Journal of biological chemistry*, *280*(28), 26448–26456.

Tormos, K. V., Anso, E., Hamanaka, R. B., Eisenbart, J., Joseph, J., Kalyanaraman, B., & Chandel, N. S. (2011). Mitochondrial complex III ROS regulate adipocyte differentiation. *Cell metabolism*, *14*(4), 537–544.

Van Der Bliek, A. M., Sedensky, M. M., & Morgan, P. G. (2017). Cell biology of the mitochondrion. *Genetics*, *207*(3), 843–871.

Von Maltzahn, J., Jones, A. E., Parks, R. J., & Rudnicki, M. A. (2013). Pax7 is critical for the normal function of satellite cells in adult skeletal muscle. *Proceedings of the national academy of sciences of the United States of America*, *110*(41), 16474–16479.

Wang, Y. X., Dumont, N. A., & Rudnicki, M. A. (2014). Muscle stem cells at a glance. *Journal of cell science*, *127*(Pt 21), 4543–4548.

Wang, S., Reuveny, A., & Volk, T. (2015). Nesprin provides elastic properties to muscle nuclei by cooperating with spectraplakin and EB1. *The Journal of cell biology*, *209*(4), 529–538.

West, A. P., Brodsky, I. E., Rahner, C., Woo, D. K., Erdjument-Bromage, H., Tempst, P., Walsh, M. C., Choi, Y., Shadel, G. S., & Ghosh, S. (2011). TLR signalling augments macrophage bactericidal activity through mitochondrial ROS. *Nature*, *472*(7344), 476–480.

White, R. B., Biérinx, A. S., Gnocchi, V. F., & Zammit, P. S. (2010). Dynamics of muscle fibre growth during postnatal mouse development. *BMC developmental biology*, *10*, 21.

Wilson, M. H., & Holzbaur, E. L. (2015). Nesprins anchor kinesin-1 motors to the nucleus to drive nuclear distribution in muscle cells. *Development*, *142*(1), 218–228.

Win, S., Than, T. A., Fernandez-Checa, J. C., & Kaplowitz, N. (2014). JNK interaction with Sab mediates ER stress induced inhibition of mitochondrial respiration and cell death. *Cell death & disease*, *5*(1), e989.

Wong, H. S., Dighe, P. A., Mezera, V., Monternier, P. A., & Brand, M. D. (2017). Production of superoxide and hydrogen peroxide from specific mitochondrial sites under different bioenergetic conditions. *The Journal of biological chemistry*, *292*(41), 16804–16809.

Yablonka-Reuveni, Z., & Anderson, J. E. (2006). Satellite cells from dystrophic (mdx) mice display accelerated differentiation in primary cultures and in isolated myofibers. *Developmental dynamics*, *235*(1), 203–212.

Yablonka-Reuveni, Z., & Rivera, A. J. (1994). Temporal expression of regulatory and structural muscle proteins during myogenesis of satellite cells on isolated adult rat fibers. *Developmental biology*, *164*(2), 588–603.

Yu, T., Robotham, J. L., & Yoon, Y. (2006). Increased production of reactive oxygen species in hyperglycemic conditions requires dynamic change of mitochondrial morphology. *Proceedings of the national academy of sciences of the United States of America*, *103*(8), 2653–2658.

Zammit, P. S., Golding, J. P., Nagata, Y., Hudon, V., Partridge, T. A., & Beauchamp, J. R. (2004). Muscle satellite cells adopt divergent fates: a mechanism for self-renewal?. *The Journal of cell biology*, *166*(3), 347–357.

Zammit, P. S., Relaix, F., Nagata, Y., Ruiz, A. P., Collins, C. A., Partridge, T. A., & Beauchamp, J. R. (2006). Pax7 and myogenic progression in skeletal muscle satellite cells. *Journal of cell science*, *119*(Pt 9), 1824–1832.

Zhang, X., Xu, R., Zhu, B., Yang, X., Ding, X., Duan, S., Xu, T., Zhuang, Y., & Han, M. (2007). Syne-1 and Syne-2 play crucial roles in myonuclear anchorage and motor neuron innervation. *Development*, *134*(5), 901–908.